University of Zurich UZH

Tree-ring records from Isla Hermite, Cape Horn: The possibility of detecting a signal of westerly winds

GEO 511 Master's Thesis

Author
Michael Thomas Kessler
14-711-816

Supervised by
Prof. Dr. Paolo Cherubini (paolo.cherubini@wsl.ch)

Faculty representative
Prof. Dr. Markus Egli

29.09.2020
Department of Geography, University of Zurich

Tree-ring records from Isla Hermite, Cape Horn: The possibility of detecting a signal of westerly winds

Author
Michael Thomas Kessler
14-711-816
michaelthomas.kessler@uzh.ch

Supervisor
Prof. Dr. Paolo Cherubini
paolo.cherubini@wsl.ch

Faculty representative
Prof. Dr. Markus Egli
markus.egli@geo.uzh.ch

Abstract

Over the last 50 years, the westerly winds of the Southern Hemisphere, a major driver of global climate, have shifted towards Antarctica and have strengthened considerably. A shift of the Southern westerly winds (SWW) is suggested to have substantially increased the ventilation of carbon-rich deep water in the Southern Ocean at the end of the last Ice Age and led to CO_2-induced warming. A better understanding of these winds is crucial to assess future developments in the climate system.

This Master's thesis applied a novel and experimental approach using tree rings to reconstruct the Southern westerly winds with focus on their decadal changes. The examined trees stem from the southernmost tip of South America (Cape Horn Archipelago) and lie within the core wind belt of the westerlies. The growth and chemical composition of these tree rings are considered to be influenced by the strong westerlies. Aside from influencing trees' physiological processes, the constantly blowing winds are assumed to transport sea salt that is taken up by the trees and archived in the tree rings. On the basis of dated tree rings, the direct method of laser ablation with focus on sodium (Na) and chloride (Cl), constituting sea salt's main components, and the indirect method of oxygen and carbon isotopes analysis were applied to retrieve a wind relevant signal.

Laser ablated sodium (Na) and chloride (Cl) signals in the tree rings present strong positive correlations with regional wind speed measurements ($r = 0.73$ and $r = 0.71$) and likely constitute a westerly winds' relevant signal. Within the isotope analysis, only the carbon isotopes show similarities with wind relevant data but the role of the winds on carbon isotopes in trees is not yet fully understood. A wind relevant signal in trees' carbon isotopes is possible. A reconstruction of the Southern westerly winds based on the laser ablated sodium (Na) and chloride (Cl) signals in the tree rings is promising, as it is comparable to an ice core based SWW reconstruction ($r = 0.49$ and $r = 0.52$). This thesis demonstrated the potential of tree-ring based SWW reconstruction, but further work and additional tree core sampling are needed to build more robust tree-ring series in order to verify these results, refine the approach and answer remaining open questions.

Table of contents

A. List of abbreviations

ACC	Antarctic Circumpolar Current
BAS	British Antarctic Survey
CDW	Circumpolar Deep Water
C. E.	Common Era
Cl	Chloride
CO_2	carbon dioxide
IRMS	Isotope-Ratio Mass Spectrometer
LA-ICP-MS	Laser Ablation-Inductively Coupled Plasma-Mass Spectrometry
Na	Sodium
RWI	Ring width index
SAM	Southern Annular Mode
SWW	Southern westerly winds

B. List of figures

C. List of tables

1   Introduction

In current times of changing climate, scientists are considering taking a more holistic approach in understanding the global climate system. Many meteorological, climatic or other yet overlooked factors contribute to global warming. When the individual role of these factors and their interplay with one other is more understood, the future consequences for our climate system can be better assessed. Surprisingly, some winds play a very essential role: The westerly winds of the Southern Hemisphere are a major driver of regional and global climate (Toggweiler et al., 2006).

Since 2013, a group from the British Antarctic Survey (BAS) has been reconstructing the strength of the Southern westerly winds by investigating lake sediments and peat records from sub-Antarctic islands (Saunders et al., 2018). The Southern westerly winds strongly influence the circulation of the Southern Ocean, which plays a fundamental role in the overall climate system. On a global scale, the Southern Ocean accounts for around 40% of the anthropogenic carbon dioxide (CO_2) uptake through the oceans and for 75% of the oceanic heat uptake (Frölicher et al., 2015). Within the ocean circulation, the Southern westerly winds drive the upwelling of carbon-rich deep-water. Stored oceanic carbon is released back to the atmosphere and atmospheric CO_2 is increased. It is suggested that a latitudinal shift in the position of the Southern westerly winds at the end of the last Ice Age has substantially increased the ventilation of deep water and triggered CO_2-induced warming (Anderson et al., 2009). The westerlies can also generate circulation conditions that favor an upwelling of warm deep water, directing warm Circumpolar Deep Water (CDW) onto the Antarctic continental shelf. This leads to a basal melting of the ice shelves and triggers big ice losses of the West Antarctic ice sheets (Holland et al., 2019; Hillenbrand et al., 2017).

Over the past 50 years, the Southern westerly winds have considerably strengthened and shifted towards Antarctica (Swart and Fyfe, 2012). This ongoing change in strength and position of the westerlies greatly influence whether the Southern Ocean will continue to act as a net carbon sink or will become an additional carbon source. Additionally, these changes of the westerlies potentially also prompt enhanced melting of Antarctic ice shelves (Le Quéré et al., 2007). Therefore, a better understanding of the Southern westerly winds is of utmost importance to better assess what future changes may occur in our global climate system.

A range of studies have already used marine and terrestrial records or other proxies to reconstruct the Southern westerly winds over millennial timescales (Kilian and Lamy, 2012). For instance, marine sediments from the Chilean continental slope, lake sediments along the windward side of the Andes and pollen records from sub-Antarctic South Georgia were used for the research. Such reconstructions provide good indications of the Southern westerly winds' behavior during the Holocene (Lamy et al., 2001; Lamy et al., 2010; Strother et al., 2015).

However, in times of changing climate and strengthening westerlies, the above-mentioned reconstructions are not of high enough resolution to derive recent climate shifts with longer decadal to centennial-scale shifts. A more recent and finer (e.g. year-to-year) resolved proxy is needed to reconstruct the

behavior of the Southern westerly winds. Trees with the methods of dendrochronology have an enormous, yet unexploited potential to fill this knowledge gap. Trees contain a comparably more recent (~ 100 years) signal with a fine annual resolution and are therefore highly suitable as a reconstruction proxy. Generally, trees act as environmental archives as the growth of their tree rings constitutes an immediate response to changing environmental conditions. The analysis of the tree rings enables to reconstruct past events or climatic factors such as temperature and precipitation.

This Master's thesis aims to apply a novel and experimental approach using tree rings from Isla Hermite (Cape Horn Archipelago) to reconstruct the Southern westerly winds. The growth and especially the chemical composition of the annually growing tree rings are expected to be influenced by the strong westerly winds. Apart from indirectly influencing the trees' physiological processes, these constantly blowing winds are supposed to stir up sea salt from the ocean and transport it to the trees. The salt spray is believed to be then taken up by the trees either through their roots, bark or leaves and be subsequently conserved in the tree rings. Apart from water and nutrients, trees also take up particles such as heavy metals or atmospheric pollutants (Liu et al., 2018; Martin et al., 2018; Hoad et al. 1992). A wind induced and archived sea-salt signal in the tree rings is assumed to vary with changes in strength or position of the Southern westerly winds. So far, no attempts have been made to reconstruct the Southern westerly winds using tree rings. At the same time, some studies have already found traces of sodium (Na^+) and chloride (Cl^-) in trees from other regions around the world (Blum, 1974; Petersen et al., 1982; Yanosky and Kappel, 1997; Yanosky et al., 1995).

1.1 Research questions

On the basis of the dendrochronological methodologies to measure and absolutely date the tree rings, the direct method of laser ablation and the indirect method of isotope analysis are used to investigate the chemical composition of the tree rings. With this approach, a reconstruction of the Southern Westerly winds is aimed to be derived. Concretely, the following research questions are addressed within this Master's thesis:

1. What analytical methods might yield some wind relevant data?

    - directly (e.g. Na^+, Cl^- or other aerosol related chemical elements or compounds)

    - indirectly (e.g. C and O stable isotopes), whose changes may be caused by changing precipitation or wind spatiotemporal patterns

2. Can a salt spray (related chemical elements) or wind signal be retrieved from the tree- ring records? How does it compare to wind relevant regional meteorological data?

3. How does a possible tree-ring based westerly winds reconstruction method compare to the more conventional marine or terrestrial record-based methods?

4. What can we expect for the future climate system based on a detectable weakening or strengthening trend of the Southern westerly winds?

2 The westerly winds

2.1 Overview

The westerly winds, shortly known as westerlies, can be found at two regions on Earth. They occur between 30° and 60° latitude in the Northern and the Southern Hemisphere. The name of the westerlies stems from the direction of their origin since they run from west to east (Pariona, 2018). The westerly winds are part of the global wind circulation system and are located between the high-pressure areas of the subtropics and the low-pressure areas over the poles (see Figure 1).
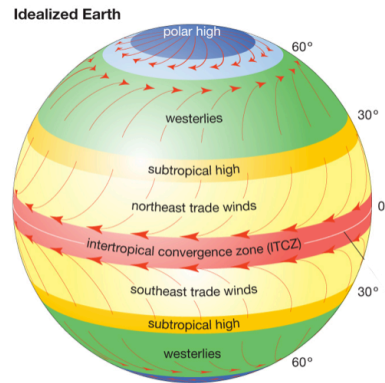
Figure 1: Existing wind circulation patterns on an idealized Earth (Source: Encyclopedia Britannica, 2019).

On the basis of the existing pressure difference between the tropics and the poles, a meridional compensating flow results from the high-pressure tropics towards the poles with lower pressures. The earth rotates to the east around its axis. Owing to the resulting Coriolis effect and to the inertia of air masses, the meridional compensating flow is deflected to the east, which finally corresponds to the prevailing west to east running wind belt of these latitudes. Historically seen, the Southern westerlies have played a convenient role for sailors or trade routes. The strong winds conditions in this area were used in order to make west to east sailing journeys faster around the Cape Horn, the most southern point of South America (Pariona, 2018). On a global scale, the Southern westerly winds are the strongest time-averaged oceanic winds (Hodgson and Sime, 2010). They reach mean wind speeds from around 1 m/s to 11 m/s respectively from around 4 km/h to 40 km/h. The strongest mean wind speeds ca be found within its core belt between 50° and 60° latitude (see Figure 2).
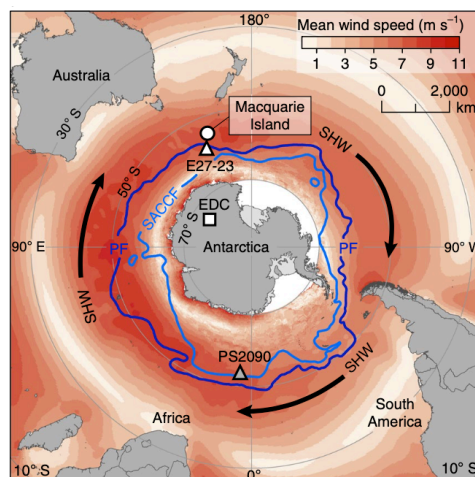
Figure 2: Mean wind speeds of the westerly winds on the Southern Hemisphere (Source: Saunders et al., 2018).

The Southern westerly winds have higher wind speeds than its northern counterpart. Land masses can basically slow down overblowing air masses. This slowing down effect does not really occur on the Southern Hemisphere because there is a lack of land masses compared to the Northern Hemisphere with a higher percentage of land masses. In addition, there exists a seasonal pattern for the Northern and Southern westerly winds. On average, during winter there are higher wind speeds measured compared to the summer. Winds are basically a compensating flow from high pressure areas to low pressure areas. During wintertime the pressure difference between the tropics and the areas over the poles is bigger that results in higher wind speeds (Pariona, 2018).

For the Southern westerly winds, there are seasonal variations identified in their position and intensity within the core belt. Owing to changes in sea surface temperatures, linked with the pressure distribution, the Southern westerlies expand during the austral winter in a northerly direction, resulting in a decrease of the intensity within its core. On the contrary, during the austral summer the Southern westerly wind belt contracts and the core intensity strengthens (Lamy et al. 2010). On a wider timescale, a 250-year periodicity could be constituted for the Southern westerly winds (Turney et al., 2016). Due to its strength and persistence, the Southern westerly winds influence the circulation of the Southern Ocean. This includes upwelling processes that control the carbon budget of the Southern Ocean or the stability of the Antarctic ice sheet, which have both great implications for our global climate system.

2.1.1 The Southern Ocean as carbon reservoir and heat sink

The Southern Ocean, denoted as the southern extremes of the Atlantic, Pacific and Indian Ocean, acts together with the Southern westerly winds as a coupled atmosphere-ocean system. The atmospheric winds drive the surface ocean current. The ocean acts a reservoir by taking up and storing carbon and heat from the atmosphere. On a global scale, the Southern Ocean plays a dominant role as it accounts for around 40% of anthropogenic CO_2 uptake through the oceans and for around 75% of the heat uptake, while only covering 30% of the total ocean surface area (Frölicher et al., 2015). (see Figure 3)
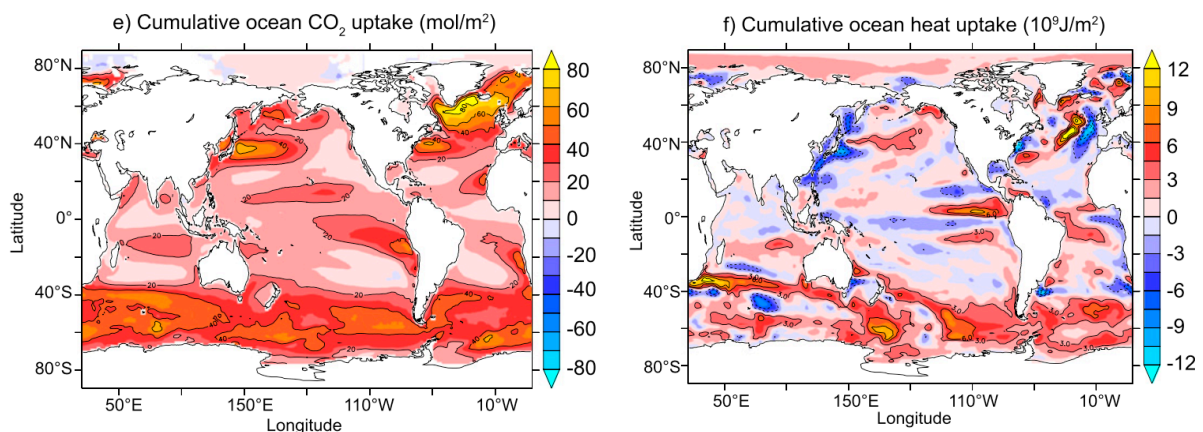
Figure 3: Cumulative anthropogenic carbon (left) and heat (right) uptake through the World Oceans between 1870 and 1995 (Source: Frölicher et al., 2015).

The Antarctic Circumpolar Current (ACC), the prevailing water current in the Southern Ocean, is driven by the main wind direction of the Southern westerly winds. Generally, water masses on the surface flow to a certain direction, resulting in a mass reduction at its origin. As a consequence, this surface mass imbalance is filled with an upward transport of deep-water, the so-called upwelling mechanism. This cold deep-water is carbon rich as it comes from the depth where the carbon in the ocean is stored and brings with that the stored carbon back to the atmosphere (Rintoul et al., 2001).

This upwelling process of carbon rich deep-water together with ocean biogeochemistry and sea ice extent control the balance of carbon dioxide (CO_2) exchanged between the atmosphere and the ocean.

As long as more atmospheric carbon is taken up by the ocean than released to the atmosphere through upwelling, the ocean acts as a carbon sink. On the contrary, when more carbon from the ocean is released through upwelling into the atmosphere than taken up, the ocean becomes a carbon source. Some models indicate that the current carbon sink of the Southern Ocean can be weakened by a strengthening and poleward shift of the westerly winds. Therefore, changes in the strength or the position of the westerlies greatly influence whether the Southern Ocean will still be a net carbon sink or become a carbon source in the future (Sigman et al. 2010; Le Quéré et al., 2007; Saunders et al. 2018).

2.1.2 Ice sheet instability of West Antarctica

It could be further observed that the Southern westerly winds also affect the stability of the Antarctic Ice Sheets. Like the upwelling of cold deep water, the latitudinal position of the Southern westerly winds can also lead to an enhanced upwelling of relatively warm Circumpolar Deep Water (CDW). This inflow of warm water onto the continental shelf results in a basal melting of the ice shelves that in turn has a stabilizing influence for the persistence of the West Antarctic Ice Sheets (see Figure 4).
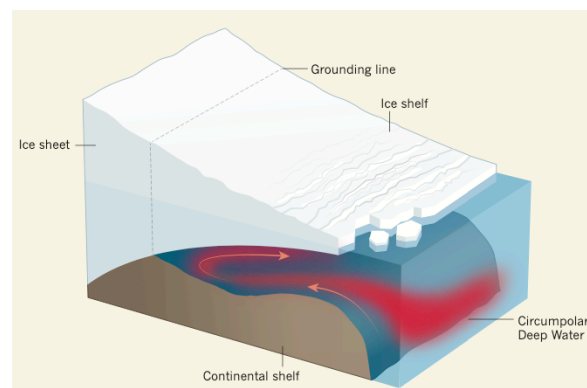
Figure 4: Schematic process of the melting ice shelf through the intrusion of warm Circumpolar Deep Water onto the continental shelf (Source: Hertzberg 2017).

This warm water inflow is believed to have led to ice-sheet retreat in the past. Hillenbrand et al. (2017) supplied first evidence for enhanced warm CDW upwelling on the basis of sediment cores from the continental shelf with foraminifera as proxy for warm water conditions in the Amundsen Sea Embayment. The warm water upwelling caused ice-shelf collapses, the ice-sheets rapidly thinned and forced deglaciation from at least 10'400 years until 7'500 years ago. The same process is understood to have been responsible for the observed continual ice loss in the region since 1940. In contrast, during the

last glacial period between 110'000 and 11'700 years ago, cooling or decreased presence of CDW or both, would have reduced melting beneath the Antarctic ice shelves and favored ice-sheet growth and stability. Holland et al. (2019) also acknowledge that wind anomalies led to enhanced import of warm CDW in West Antarctica and caused the loss of ice. However, they go one step further and link the changes in the winds to some part to human-induced global warming, along with shorter-term natural climate variations. Increased greenhouse gases caused wind anomalies that are in turn favorable for enhanced warm water upwelling. All in all, this wind driven upwelling of cold or warm deep water shows that the Southern westerly winds have great implication on the future of the Southern Ocean as a carbon sink and the continuing melting of the Antarctic Ice Sheet. Therefore, it is of utmost importance to better understand the past westerlies' behavior on the basis of proxy reconstructions.

2.2 Reconstructions of the Southern westerly winds

A range of studies have attempted to reconstruct the behaviour of the Southern westerly winds on the basis of various records. For that, particularly marine sediments, terrestrial records or biological proxies have been used (Saunders et al., 2015; Kilian and Lamy, 2012). For instance, the iron concentration in marine sediments from the Chilean continental slope or biogenic carbonate accumulation rates in lake sediments along the windward side of the Andes were investigated (Lamy et al., 2001; Lamy et al., 2010). In general, these proxies are linked to a climate variable (e.g. precipitation, temperature) and with the help of the proxy's behaviour, a climate variable record (e.g. rainfall variability) can be established. The modern relationship between the climate variable and the Southern westerly winds is then used to conclude about the past changes of the westerlies' behaviour. A reconstruction of the westerlies can also be derived in a more direct manner with biological pollen for example. In subantarctic South Georgia, observed increases in long-distance and non-native pollen grains could be denoted to stronger westerlies during certain times (Strother et al., 2015).

2.2.1 Paleoclimate records: Last glacial maximum and Holocene

In recent time, there is evidence that the Southern westerly winds have strengthened and shifted toward Antarctica over the past 50 years (Toggweiler, 2009). It is thought that this strengthening and shift occurred as a response to the warming that stems from elevated carbon dioxide concentrations in the atmosphere (Gillett et al., 2003; Shindell and Schmidt, 2004). Something similar seems to have happened at the end of the last Ice Age, 17'000 years ago: Earth's temperature warmed, atmospheric carbon dioxide increased, and the Southern westerlies appear to have shifted toward the pole (Toggweiler et al., 2006; Lamy et al. 2007). In contrast, it is also proposed that the poleward shift of the westerlies 17'000 years ago has happened before the warming. A shift of the westerly winds has caused an increase in atmospheric carbon dioxide that contributed to the warming. It is suspected that the accumulated carbon dioxide in the atmosphere have been released from the Southern Ocean through westerly wind-driven upwelling of carbon-rich deep water (Anderson et al. 2009). It is still controversially discussed whether the underlying mechanism of the Southern westerly winds' shift and

strengthening was as a response to elevated atmospheric carbon dioxide or whether shifted and strengthened westerlies themselves caused atmospheric carbon dioxide to increase (Toggweiler, 2009). However, the intensification and southward shift of the westerlies 17'000 years ago is well known and evident in paleoclimate reconstructions. Koffman et al. (2014) provide a reconstruction of the Southern westerly winds together with an overview of important paleoclimate proxies. They reconstructed the behaviour of the westerlies with dust particles, investigated in ice cores of West Antarctica (see Figure 5).
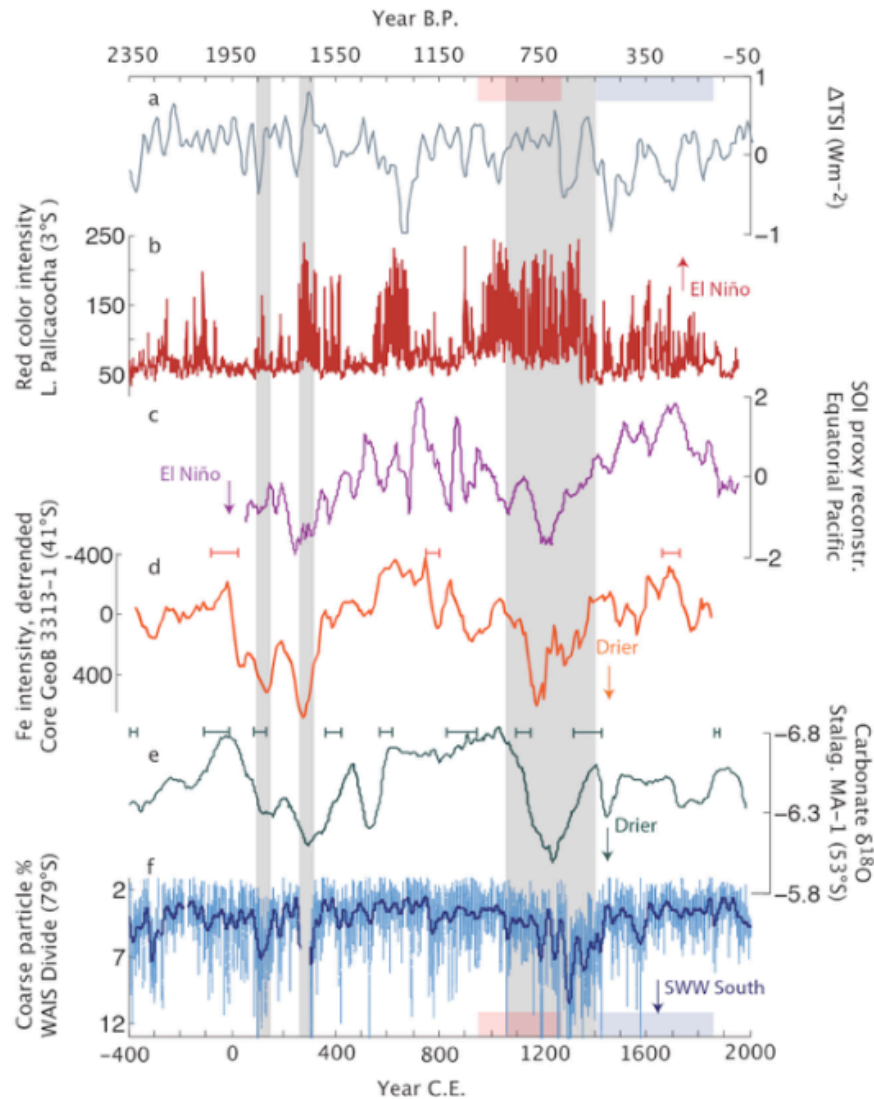
Figure 5: "*Paleoclimate reconstructions from the eastern Pacific region: (a) Change in total solar irradiance (TSI) based on variability of cosmogenic [10]Be, the production of which is modulated by the strength of the open solar magnetic field (Steinhilber et al., 2009). (b) Red color intensity record of sediments from Laguna Pallcacocha, Ecuador; greater color intensity indicates more El Niño-driven high precipitation events (Moy et al., 2002). (c) Southern Oscillation Index (SOI) precipitation-based reconstruction; negative values indicate a more El Niño-like state (Yan et al., 2011). (d) Detrended iron intensity record from marine sediment core GeoB 3313-1 on an inverted axis (Lamy et al., 2001). Lower values suggest more humid conditions. Orange error bars indicate published ^{14}C age control points and associated 1σ AMS analytical error (F. Lamy, personal communication of the author, 2014). (e) δ^{18}O of stalagmite MA1 on an inverted axis. Lower values indicate an increased drip rate, driven by higher precipitation (Schimpf et al., 2011). Green error bars show positions and 2σ error of U/Th ages. (f) WAIS Divide coarse particle percentage on an inverted axis, using timescale WDC06A-7. Data sets are plotted on their own published timescales. Gray bars indicate intervals of inferred southerly position of the SWW in the eastern Pacific, based on our interpretation of the CPP and South American precipitation reconstructions. Red and blue bars indicate the MCA and LIA intervals, respectively"* (Source: Koffman et al., 2014).

Aside from this southward shift 17'000 years ago, a more southerly position with stronger core wester-lies could be identified for the period of 260-310 C. E. and during the Medieval Warm Period (1050-1400 C. E.). The westerlies seem to have occupied a more northerly position with weaker core winds during the Little Ice Age (1400-1430 C.E.) and remained in this position until 1850-1950 C. E.

2.2.2   Recent shift and strengthening

In recent times since 1950 C. E., the Southern westerly winds have shifted southward and substantially strengthened (see Figure 6). This trend can also be seen with the Southern Annular Mode (SAM) in-dex. It is a station-based index that describes the zonal pressure difference between the latitudes of 40°S and 65°S. Positive SAM index values relate to weaker than average westerlies in the mid-latitudes (30°-50°S) and stronger westerlies over the mid-high latitudes (50°-70°S) (Marshall, 2003).
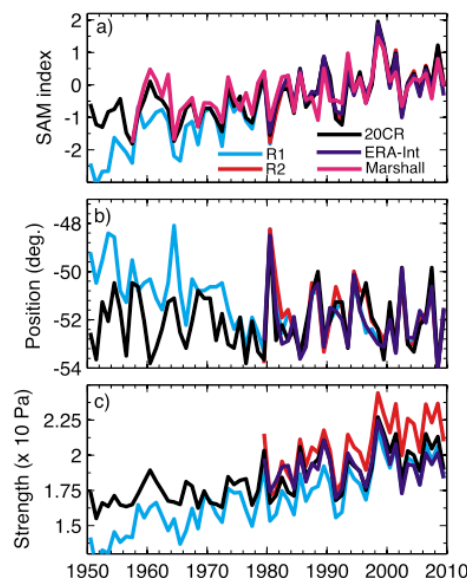
Figure 6: Changes (a) in the annual mean Southern Annular Mode (SAM) index, (b) in the surface Southern westerlies lati-tudinal position and (c) strength of the zonal mean wind-stress for four reanalysis products (Source: Swart and Fyfe, 2012).

The strengthening trend towards the end of the 20th century is also visible in the ice core-based recon-struction of Koffman et al. (2014). A southward shift of the westerlies makes them stronger; coarser dust particles are transported and therefore particles of bigger sizes can be found in the ice cores of West Antarctica. On the contrary, when the westerlies are shifted northward, the winds are weaker, more fine dust particles are transported and smaller particles can be detected in the ice cores.
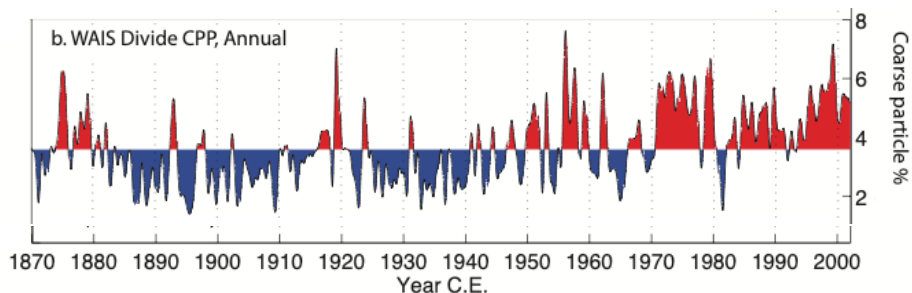
Figure 7: Magnified view of curve f from Figure 5. West Antarctic Ice Sheet (WAIS) Divide coarse particle percentage on the y-axis over the period (1870-2000) on the x-axis. Delineations in red and blue from the mean of the record over the given time period (Source: Koffman et al., 2014).

3 Dendrochronology: Trees, wind and salt

The science of dendrochronology includes the dating of tree rings to the exact year when the tree rings were formed. Trees act as environmental archives as the growth of their tree rings is an immediate response to the surrounding environmental conditions. Based on the analysis of the information content in dated tree rings, historical and environmental question can be examined. In the subfield of dendroecology, dated tree rings are used to study the environment and ecological problems: Tree decline in forests, reconstruction of temperature and precipitation or disturbances for trees such as insect outbreaks, fires or heavy winds (Kaennel and Schweingruber, 1995).

Winds can cause considerable physical damage to trees as they can abrade, defoliate them, break branches or even completely bend them (Coutts and Grace, 1995). While wind-induced physical damages are an important issue, the focus within this approach lies on the winds' role of transporting airborne particles to the trees and their indirect role of affecting trees' physiological processes such as photosynthesis or transpiration.

3.1 Particles uptake of trees and the characteristics of sea salt

Aside from water and nutrients, trees also take up heavy metals and are capable of taking up pollutants from the atmosphere (Liu et al., 2018; Martin et al., 2018; Hoad et al. 1992). Generally, particles enter the tree through its roots by absorbing soil water or through the stomata of its leaves by assimilating gaseous compounds (Cocozza et al., 2019). Moreover, the bark of a tree, constituting the interface between the plant and the environment, also appears to incorporate parts of airborne particles as increased concentrations of mercury were measured (Chiarantini et al. 2016).

Up untill now, only few attempts have been made to directly detect salt in trees. Few studies could identify sodium (Na^+), chloride (Cl^-) and reduced tree-ring growth in trees that grew near to streets where de-icing salt was used for the roads' safety in winter (Blum, 1974; Petersen et al., 1982). In addition, chloride concentrations were determined within the rings of trees which were located in proximity to a salt-solution mining field or which grew in a saltwater intrusion influenced estuary (Yanosky and Kappel, 1997; Yanosky et al., 1995). Additionally, increased sodium (Na^+) and chloride (Cl^-) contents could be measured in leaves of trees that were irrigated during the growing season with salt containing water or sodium and chloride cations could be detected in cotton leaves that were exposed to simulated salt dust storms (Ziska et al., 1991; Abuduwaili et al., 2015).

In nature salt occurs as sea salt in oceans. Seawater has on average a salinity of around 3.5% with sodium (Na) and chloride (Cl) as the most abundant salts in the ocean. They often build together sodium chloride (NaCl), which is the major component of sea spray. Aside from Cl^- (55%) and Na^+ (30.6%), sea salt further contains minor components of SO_4^{2-} (7.7%), Mg^{2+} (3.7%), Ca^{2+} (1.2%), K^+ (1.1%) and other elements (0.7%). Figure 8 shows that sea salt particles range in size from less than one micrometer up to several micrometers (EEA, 2012; Tomasi and Lupi, 2017; Millero et al., 2008). If wind-driven particles are taken up by trees, the winds would directly influence the abundance of the particles in the tree rings.
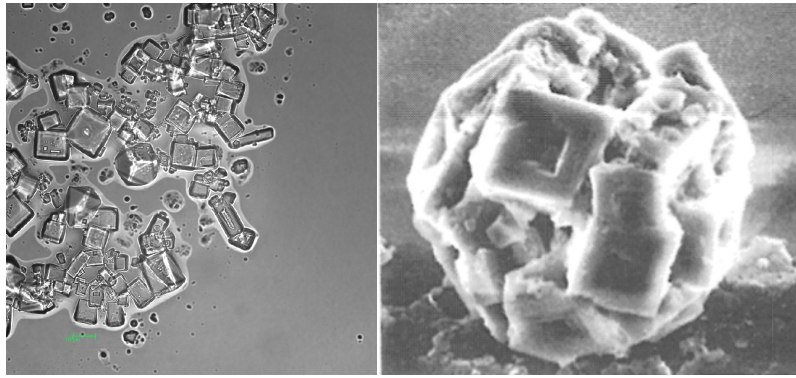
Figure 8: Sea salt (left) and a single sea salt particle (right) with a diameter of 30 μm (Source: NASA, 2009; Pruppacher and Klett, 1997).

3.2 The indirect influence of wind on trees

The surrounding environmental conditions of a tree can be influenced by winds and with that the tree's physiological processes such as photosynthesis or transpiration can change. As a result, winds indirectly influence the composition of oxygen or carbon stable isotopes in tree rings. Isotopes are atoms of a chemical element which have the identical number of electrons and protons but differ in the number of neutrons. Therefore, isotopes represent the same element but have different mass numbers such as the light (^{12}C) and the heavy (^{13}C) carbon isotope. As they vary in weight and occur in different frequencies, isotopes are used to investigate and understand physiological processes (Treydte, 2019).

The level of stable carbon isotopes in tree rings is influenced by the rates of stomatal conductance and photosynthesis (McCarroll and Loader, 2014). Warm and dry weather conditions with low water ability promotes the closure of the stomata and less CO_2 is taken up. The intercellular CO_2 concentration is reduced and relatively enriched with the heavier carbon isotope, which increases the δ^{13}C value in the tree rings. On the contrary, cool and wet weather conditions with high water ability keeps the stomata open and CO_2 is taken up. The intercellular CO_2 concentration is then relatively enriched with the lighter carbon isotope and the δ^{13}C value in the tree rings is decreased (Kubota et al., 2017; Treydte, 2019). Comparatively, the stable oxygen isotopes are controlled by the stomatal conductance. In addition, the δ^{18}O value in tree rings resembles the signal of the source water of the tree as rainwater, groundwater or meltwater have different isotopic signals (Vuaridel et al., 2019).

However, the role of winds on these physiological processes is still not fully understood. It is implied that higher wind speeds induce greater transpiration rates that lead to a greater water stress for a tree (Bidwell, 1979). On the other hand, there are indications that wind can reduce transpiration (Dixon, 1984). Moreover, some studies implicate that the effect of wind on plants is modified by the behaviour of the stomata. In response to the shock of wind, the stomata may shut (Caldwell, 1970) or even open more widely (Grace, 1974). Winds can also cause stomatal damage that could lead to greater water loss (Wilson, 1979). Besides the winds, salt can also lead to a further physiological stress for a tree. It could be shown that trees immersed in seawater did not show altered levels in δ^{18}O but higher δ^{13}C values which were likely caused by osmotic stress from the root immersion in saltwater (Kubota et al., 2017).

4   Study area

4.1   Isla Hermite, Cape Horn

The study area lies in southernmost Tierra del Fuego, more precisely in the Cape Horn region, on Isla Hermite (55° 50' S, 67° 25' W). Together with six other islands it builds the inhabited Hermite Archipelago, part of the Chilean commune Cabo de Hornos and is located around 110 km south of Ushuaia (Argentina). Isla Hermite is the biggest island with a surface area of around 144 km^2, whereas Isla Hornos is the most famous island with the Cape Horn that is usually considered as the southernmost point of South America (Wikipedia, 2015) (see Figure 9).

Figure 9: Overview of Isla Hermite within the Cape Horn Archipelago in southernmost South America (Source: Australis, 2017; Rolfo and Ardrizzi, 2013).

Due to its size and location within the core belt (50 - 60°S) of the Southern westerly winds, the British Antarctic Survey (BAS) conducted an expedition to Isla Hermite in 2015 (see chapter 5.1 Sampling during BAS expedition of 2015). The aim was to study lake sediments and peat records in order to reconstruct the strength of the Southern westerly winds. During this expedition also core samples from seven *Nothofagus antarctica* trees were taken.

4.2   Climate and vegetation of Tierra del Fuego

The climate of southern Tierra del Fuego is strongly influenced by the existing southern Andean foothills and the conditions in the Southern Ocean and the Antarctic. The climatic conditions are characterized by low temperatures and strong winds throughout the year. Generally, three climate types can be distinguished in this heterogenous region: rainy cold temperate climate (western windward parts under the influence of Pacific with wet air masses), high-altitude ice climate (elevated parts of the southern Andean foothills) and tundra climate (eastern parts in the rain shadow with dry air masses).

The Hermite archipelago, located in the southeast, have a tundra climate with the subtype of sub Antarctic maritime climate with low rainfall. Due to the influence of the surrounding Pacific Ocean and the southern Drake Passage, relatively constant temperatures throughout the year are the consequence. The average temperatures in this region are around 8 °C in summer and 4 °C in winter. The nearest precipitation measurement station in Puerto Williams on Navarino Island, 90 km north of Isla Hermite, achieves a yearly rainfall of around 448 mm (Heusser, 1989; Biblioteca del Congreso Nacional de Chile, 2020; Xercavins Comas, 1984).

The existing climate in Tierra del Fuego further determines the prevalent vegetation of this region. Across Tierra del Fuego, four different southeasterly trending vegetation zones are differentiated. Starting from the north, the steppe is followed southward by deciduous beech forest that devolves in an evergreen beech forest and ends with the Magellanic moorland or tundra in the south (Heusser, 1989). The Hermite archipelago is part of the southernmost vegetation zone, the Magellanic moorland or tundra. The Hermite islands are composed of mountainous terrain, but altitudes do not exceed 500 meters. The vegetation is characterized mainly by moorland and scrub formation where occasionally trees of *Nothofagus antarctica* and shrubs grow (see Figure 10) (Ponce and Fernández, 2014).

Figure 10: Moorland vegetation (left) and *Nothofagus antarctica* tree (right) on Isla Hermite during the BAS expedition of 2015 (Pictures: Eñaut Izagirre).

Nothofagus, known as the false or southern beech, is a genus that can only be found in the Southern Hemisphere. Its 34 species are present across southern South America, southeast Australia and Tasmania, New Zealand, New Guinea and New Caledonia. The species *Nothofagus antarctica* is a native of temperate South America and is of interest for this Master's thesis. The species' distribution spans from Cape Horn through the Andes to around 500 kilometers south of Santiago de Chile. Typically, it occurs from sea level to 1'500 meters elevation and survives in the widest range of habitat types: Areas of low temperature, poor soils, steep slopes, in marshes at higher altitudes or dry sites near the Patagonian steppe. Basically, it is usual at sites that are too harsh for most other tree species. *Nothofagus antarctica* can appear both as a tree and as a shrub. However, the shrub form is more common in the northern regions and the tree form more towards the southern regions. The leaves of the tree are typically one to three centimeters long and are broadly ovate to triangular or heart-shaped (Jones, 2020; Veblen et al., 1996)

4.3   Southern westerly winds, sea salt and trees on Isla Hermite

This Master's thesis approach expects that the Southern westerly winds transport sea salt onto Isla Hermite and to the *Nothofagus antarctica* trees. The oceans comprise the major source of sea salt aerosols as they are formed and emitted from the ocean's surface to the air through wind stress. Sea salt aerosols, which are a suspension of fine solid salt particles or liquid droplets in air, follow a bubble-burst mechanism (see Figure 11). As air bubbles move upward to the ocean's surface, their film thins, and it bursts into small fragments and drops. The salt particles remain in the air as the drops evaporate (Pruppacher and Klett, 1997).
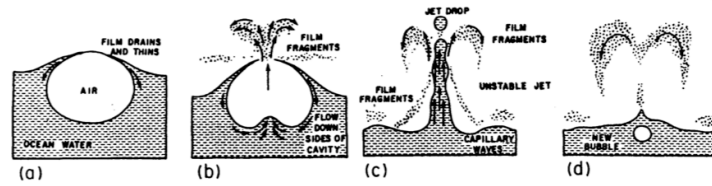
Figure 11: Different steps (a-d) in the sea salt aerosol formation at the oceans' surface (Source: Pruppacher and Klett, 1997).

Within this formation process, the sea salt aerosols are stirred up over the ocean and are supposed to be then transported as salt spray by the westerlies onto the island (see Figure 12).

Figure 12: Assumed sea-salt spray transported by the Westerly winds onto the island indicated with yellow arrows.

Given that sea salt particles range in size from less than one micrometer up to some micrometers and salt could already be detected in trees, part of the oceanic salt spray is suspected to be taken up by trees, located near the shore. This uptake is assumed to work either through the roots, the stomata of the leaves or through penetration of the bark. Subsequently, the possible taken-up sea-salt is expected to be conserved and archived in their annually growing rings. This archived sea-salt signal would allow to reconstruct the westerly winds as the signal is supposed to vary over the years with changes in strength or position of the winds.

5   Material and methods

The taken tree cores during the BAS-expedition of 2015 build the sample basis of this approach. The material and methods further involve the dendrochronological methodologies to measure the tree-ring widths of the samples with the corresponding equipment (Rinntech TSAP-Win software) and to absolutely date the trees by applying the crossdating principle. On the basis of these measurements, some advanced instrumentations are further used to directly (laser ablation) and indirectly (mass spectrometry) analyze the chemical composition of the tree rings with a focus on sodium (Na^+) and chloride (Cl^-) respectively the oxygen ($^{18}O/^{16}O$) and carbon ($^{13}C/^{12}C$) stable isotopes.

5.1   Sampling during the BAS expedition on Isla Hermite in 2015

The British Antarctic Survey (BAS) conducted a three-weeks expedition to Isla Hermite, starting in the end of February and ending in the beginning of March 2015. The aim was to rebuild sea spray and aerosol deposition by investigating lake sediment and peat records in order to reconstruct the strength of the Southern westerly winds (BAS, 2015). Therefore, the working area was located in the north-western low-lying part of Isla Hermite where the prevailing westerly winds hit the land as freely as possible (see Figure 13).
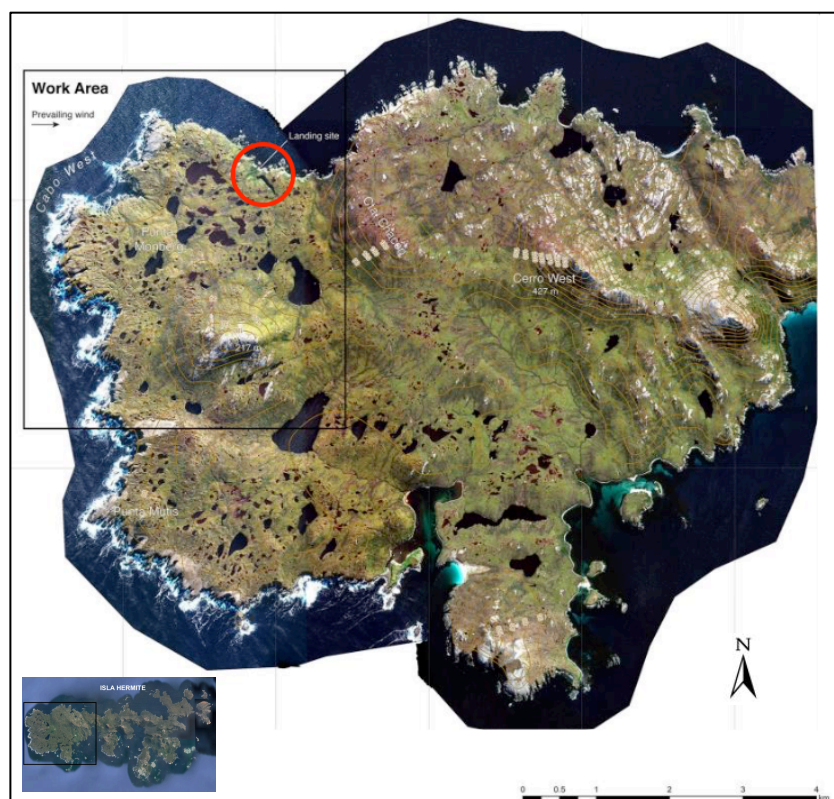
Figure 13: Overview of the western part of Isla Hermite with the work area of the BAS during the 2015 expedition indicated with the black rectangle and the location of the taken tree cores of *Nothofagus antarctica* marked with a red circle (Source: BAS, 2015; Google Earth).

During this expedition core samples from seven coastal *Nothofagus antarctica* trees were taken. They build the samples basis of this Master's thesis and are from a dendrochronological perspective highly valuable since they grew in an extremely remote region. Very likely they are from the most southern

living trees on this planet. The samples were taken using a light-weight tree corer which takes out a slim core section without killing the tree. The corer is inserted into the tree by turning it clockwise with a bit of pressure. When the trees' mark is reached, the tree core section can be taken out with the help of an integrated cutter and a metal stick (see Figure 14).

Figure 14: Tree core sampling using a tree corer on a coastal *Nothofagus antarctica* tree on Isla Hermite (left) and a taken-out tree core section on the metal stick (right) by the BAS in 2015 (Pictures: Eñaut Izagirre).

The selection of trees was limited since they are sparsely growing on Isla Hermite. Nevertheless, trees located as close as possible to the shore of the ocean, were selected and cored. The distances for the trees measure between 100-188 meters from the ocean (see Figure 15).
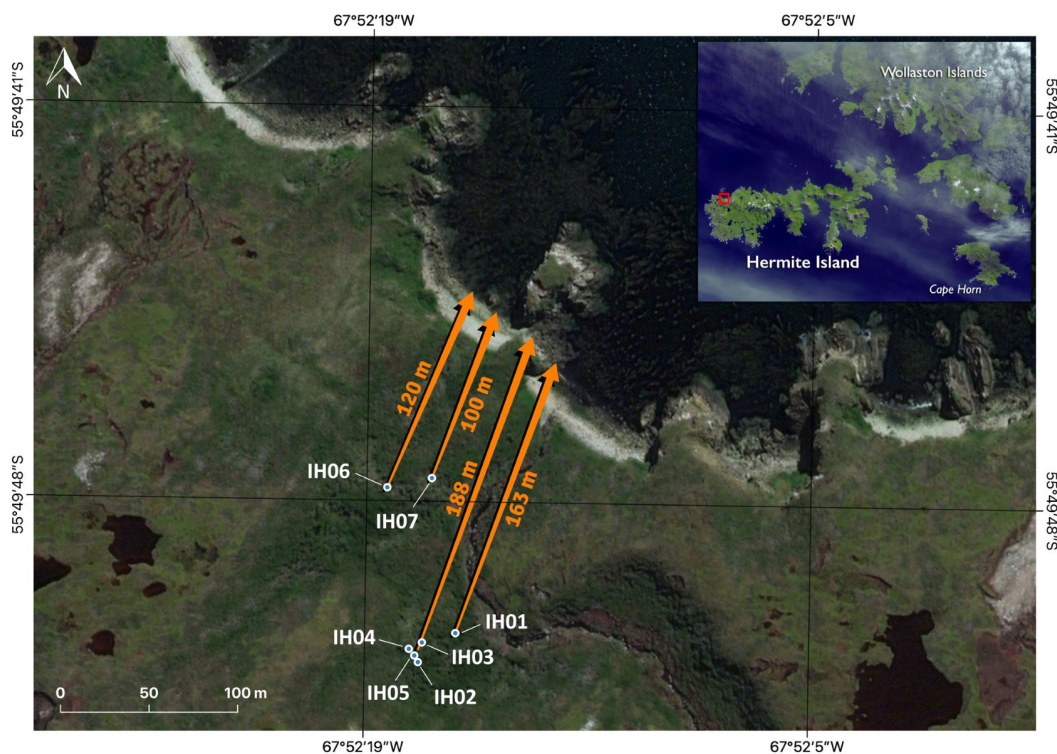
Figure 15: Overview of the location of the *Nothofagus antartica* trees on Isla Hermite (Background image: Digital-Globe/GeoEye-1 image available through QGIS 'QuickMapServices' plugin). Inset figure shows the location of Isla Hermite on the Hermite archipelago, close to Cape Horn (Source: ASTER Terra satellite image from 20 September 2005, by NASA).

The sample set consists of seven tree cores from coastal *Nothofagus antarctica* that are between 10-15 cm long and have a diameter of 1 cm. Further information and pictures of the sample set can be found in the appendix (see 10.1 Sampling details of the BAS-expedition in 2015).

5.2 Preparation in the laboratory

A core-microtome developed by Gärtner and Nievergelt (2010) was used to prepare a plain surface on the tree cores to enhance the visibility of the tree rings for the width measurement. Therefore, each sample was fixed in the sample holder with its wood fibres in a vertical direction (see Figure 16).

Figure 16: Core-microtome with the sample IH05 fixed in the sample holder under the overlying knife holder (red).

The knife holder with the clamped cutter is operated manually, carefully moving it on the metal sledge guidance over the top layer of the fixed wood sample. In the figure shown, the uppermost wood layer is removed through the cutter and the knife holder has to be returned to its initial position afterwards. Before the cutter can be moved again to remove the uppermost wood layer, the lead screw on the bottom needs to be turned. This moves the sample holder with the fixed sample in an upward direction and allows again the uppermost wood layer to be cut. This procedure was repeated until a wide and plain enough surface on the tree core was generated that made the tree rings visible. Adding water on the wood surface would simplify the cutting process, however this was on purpose avoided since with that the sea-salt within the tree rings could have been washed out. To enhance the visibility of the tree rings a fine sanding paper (15 μ) was further used. In order to avoid a smearing of the chemical signal, the sample surface was very carefully grinded in parallel direction to the tree rings.

5.3 Tree-ring width measurement

At the start of the measurement, the samples were placed under the microscope and the tree rings were counted backwards starting from the outermost ring near the bark in order to simplify the later tree-ring width measurement. With the help of a needle every decade was marked with a dot, every fifty years with two dots and every millennium with three dots within the corresponding tree ring. The outermost ring near the bark was defined as the year 2015 since the samples had been taken on the Southern Hemisphere at the end of February 2015 during the austral summer. Generally, a tree builds latewood cells that complete a tree ring towards the end of the growing season at the end of the summer. The growing season for trees in the Tierra del Fuego region terminates around the end of February (D'Arrigo and Villalba, 2000). Based on that, assumptions were made that the tree ring of 2015 had already been completed in this tree cores and was therefore considered as the outermost ring. In

tree cores where the outermost ring seemed not to have been fully completed, the measurement was started with the next fully completed ring and this ring was considered as the one of 2014. The tree-ring width of the cores was then measured with the help of Rinntech TSAP-Win software. The computer was connected to a Rinntech LINTAB table, which could be moved with a crank. The samples were placed on this movable table consecutively (see Figure 17).
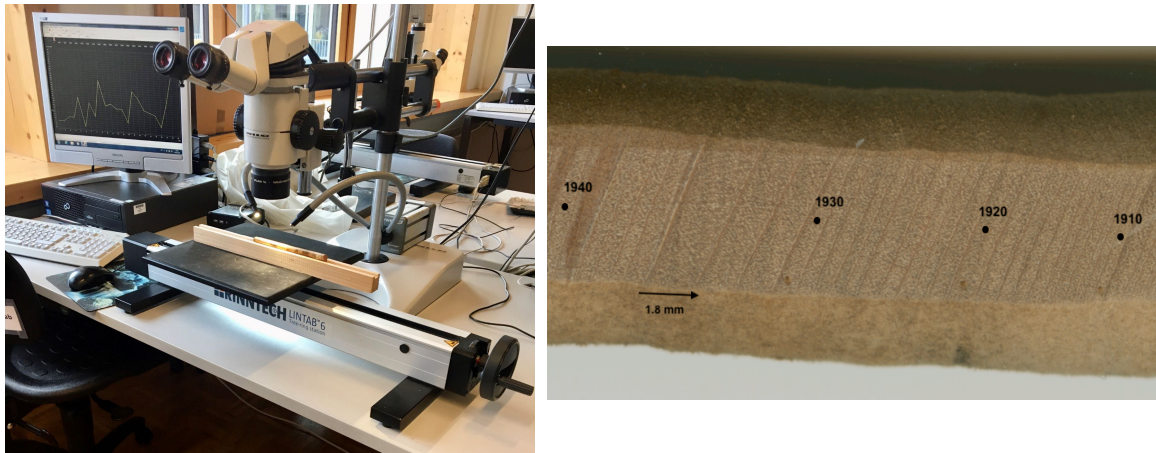
Figure 17: Rinntech TSAP-Win user interface on the computer screen with microscope, linked movable Rinntech LINTAB table and sample on the table (left). Magnified view on the sample surface IH01 for the tree rings of 1940-1910 (right).

Afterwards, the tree cores were examined from above with a magnified view through a microscope, which had a crosshair at its focus. Whenever the crank was turned, the table moved, and the crosshair was shifted from one tree ring to the next tree ring within the core. When the crosshair reached the end of a tree ring, the new ring border was registered with a mouse click. At the same time, the movement of the table was detected by the software and converted into a ring width (10^{-2} mm). The measurements were conducted from bark to pith, and the edge of the latewood was defined as the ring border. When the pith was reached, the age of the sample was calculated automatically.

The next step was to crossdate the measured tree-ring width curves within this samples size. The crossdating procedure aims to assign the individual tree rings of a sample to the exact calendar year when the rings were formed by matching variations in tree-ring width. Certain years within a geographic location are known to have a pronounced growth of tree rings (e. g. really narrow or broad rings). Therefore, such so-called marker years are used to better match common patterns in tree-ring widths (Douglass, 1941; Kaennel and Schweingruber, 1995). To practically crossdate the samples, the curves of the measured tree-ring widths are displayed on the computer screen with the Rinntech TSAP-Win software. The curves of the different cores were then visually compared, looking for similar patterns of broad and narrow rings. On the basis of common tree-ring width patterns, the curves could be temporarily shifted. The plausibility of such temporal shifts was then checked by assessing the rings of the samples under the microscope again. This procedure is necessary so that any false and missing rings could be identified and be corrected by inserting, deleting a ring or measuring parts again.

5.4   Laser ablation

The direct method of Laser Ablation-Inductively Coupled Plasma-Mass Spectrometry (LA-ICP-MS) was selected to analyze the chemical composition of the tree rings. It is particularly applied within geological, biological or medical studies for the direct analysis of solid samples. This method can also be used for dendrochronological purposes as it is a non-destructive approach and is highly suitable for narrow tree rings (Loader et al., 2017). The tree cores were analyzed by using LA-ICP-MS at the laboratory of the Institute of Geochemistry and Petrology at the ETH Zurich.

The procedure within this coupled three parts technique is straightforward. In the first part, a laser beam is focused into the surface of the sample and an aerosol of the constituents is produced through the ablation process. The aerosol is then transferred by a gas stream, to the second part, the high-energy Inductively Coupled Plasma. As it passes there through the ion source of the instrument, it is atomized and ionized. The resulting ions are then transferred through interface cones and primary beam optics to the third part, the Mass Spectrometer. The intensity of the elements of interest are measured and these signal intensities correspond then to the abundance of the investigated elements in the initially ablated sample (Fernández et al., 2007; Tofwerk AG, 2017).

Within this approach, the focus lies on the trace elements that constitute main components of sea-salt, in particular sodium (Na^+) and chloride (Cl^-) as well as some minor components like magnesium (Mg^{2+}), calcium (Ca^{2+}) and potassium (K^+). Given that the available laser shots are limited to 500 for a single measuring run, the measurements were carried out on the four tree cores that have suited each other the best during the crossdating process. The four samples had to be prepared and fixed with springs and screws together with a standard reference material of common trace elements on a plate. The laser beam is stationary and the sample on the plate can be moved in x, y, and z directions with installed high-precision motors in the sample stage (see Figure 18).

Figure 18: The fixed four tree core samples IH01, IH03, IH04 and IH05 together with a standard reference material on the measuring plate viewed from above.

The analysis was performed in each tree ring starting from 1900 until the last tree ring of 2014/2015 for the four tree cores. The laser was operated a pulse rate of 5 Hz with a laser energy of 2 J/cm^2. Backgrounds were measured for 20 seconds prior to each ablation. The ablation time was 40 seconds followed by a wash out of 20 seconds. A circular spot with a beam diameter of 74 μm and a depth of

around 1 mm was chosen to ablate within the tree rings. The size of the laser spot was determined by the smallest tree ring with a width of 80 μm. Each spot was placed in the middle of the tree ring in the earlywood, since it was not clear where within the year the sea-salt signal was to be expected. The location of the signal within the tree rings is dependent on the yet unknown predominant uptake mechanism through roots, leaves or bark. The allocation of the spots was manually performed on a screen and programmed with a computer (see Figure 19).
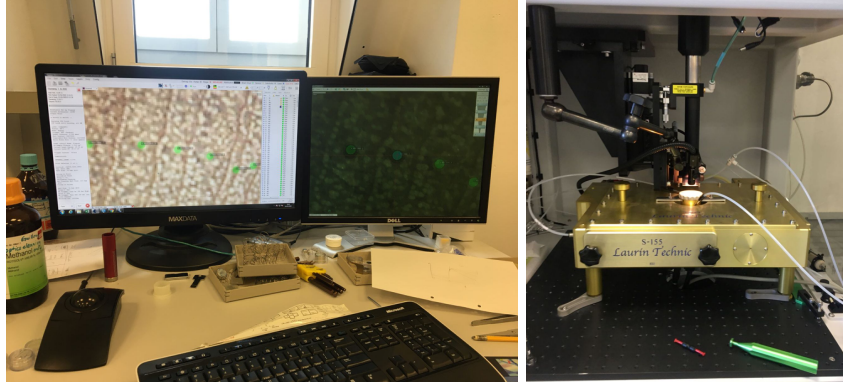
Figure 19: The screens to select the location of the laser spots within the tree rings of the samples (left) and the sample stage with the incoming laser beams from above (right).

Given that sodium (Na) is everywhere available a high intensity is expected. For chloride a low intensity is expected due to its high Ionization energy. For data reduction, Sills software developed by Guillong et al. (2008) was used to remove spikes, select integral intervals and calculate net count rates for the measured elements. This count rates were normalized to ^{13}C in order to correct for differences in ablation yield. A normalization procedure applied by Perone et al. (2018) was used to make the different intensities of the elements comparable. This normalization is based on common temporal levels for the different elements independently of each other in the tree rings of the four samples. An index value between 0 and 1 was assigned for each year for a specific element by using the subsequent equation:

$$(I_x) = (level_x - level_{lowest}) / (level_{highest} - level_{lowest})$$

where $level_x$ refers to the measured intensity of a specific year, $level_{lowest}$ and $level_{highest}$ refer to the lowest and highest intensities measured for the specific element within the tree rings of four samples.

5.5   Isotope analysis

The indirect method of isotope analysis was applied to derive possible wind relevant data from the tree core samples. The focus relies on the carbon and oxygen stable isotopes. Six of the seven tree cores were used for this analysis. Sample IH02 was not used since it only provides a short time record. First, the six tree cores were split in blocks of five years with a scalpel under the microscope (see Figure 20). This block approach was chosen because a yearly ring splitting was not possible due to the narrow rings of the samples, resulting in a total of 154 block samples. Subsequently, each of these split block samples was separately ground with a centrifugal mill. The resulting powdery material was then individually packed in Teflon bags to conduct a cellulose extraction. For this isotopic analysis, particularly

the cellulose components of the wood are of interest since in these components generally the better climate signal can be found. This applies especially to time series that are longer than 50 years as the wood composition (amount of cellulose/lignin) can considerably change over time (Gray and Thompson, 1977). In order to extract the cellulose components from the wood, the Teflon bags were placed together with two solutions (first sodium hydroxide, then sodium chlorite) in Erlenmeyer flasks and held in a 60°C warm water bath for 17 hours. As a last preparation step, the extracted cellulose material, yielding around 35-45 % of the former mass, was individually weighed (1± 0.05 mg) and packed in silver capsules. For the isotope analysis an Isotope-Ratio Mass Spectrometer (IRMS) was used. The measuring principle comprises that the silver capsules with the cellulose material are combusted and ionized. The resulting gas is then accelerated over a potential that separates the stream of ions according to their masses. Heavier ions are deflected at a bigger radius and lighter ions at a smaller radius. Based on this principle and using a measuring detector, the percentage share of the lighter and heavier carbon and oxygen stable isotopes can ultimately be determined (Rodrigues et al., 2013).

Figure 20: The different preparation steps for the isotope analysis (from left to right): splitting the tree cores in blocks of five years with a scalpel under the microscope, milling the block material with the centrifugal mill, packing of the powdered wood material in Teflon bags, the cellulose extraction process in the warm water bath and the final packing of the extracted cellulose material in silver capsules.

5.6   Meteorological and reconstruction data

The wind relevant meteorological data was obtained from different sources. The SAM index data stems from long-term station-based measurements (Marshall, 2003). Wind speed measurements of Ushuaia are based on an operated weather station and the data was accessed through personal communication with Bianca Perren from the British Antarctic Survey. The reanalyzed wind speed measurements of Isla Hermite were retrieved from the KNMI Climate explorer that collects and provides climate data analysis tools. An average box of 1-2° around Isla Hermite was used to retrieve zonal winds from reanalysis data (KNMI, 2020). Altogether, these wind relevant data was chosen since there is a lack of data for this remote region but it was aimed to cover global data (SAM index), regional data from a regularly operated weather station (wind speed measurements of Ushuaia) and local data from the study site (Reanalysis wind speed measurements around Isla Hermite). The ice core based SWW reconstruction is obtained from Koffman et al. (2014) and the raw data of this study was given by the author for the purpose of this thesis.

6 Results

6.1 Tree-ring width measurement

The tree-ring widths of the seven samples and their middle curve are depicted in Figure 21. The tree-ring width measurements of the individual tree cores can be seen in the appendix (see 10.2 Tree-ring width measurements of the samples).

Isla Hermite Tree Cores
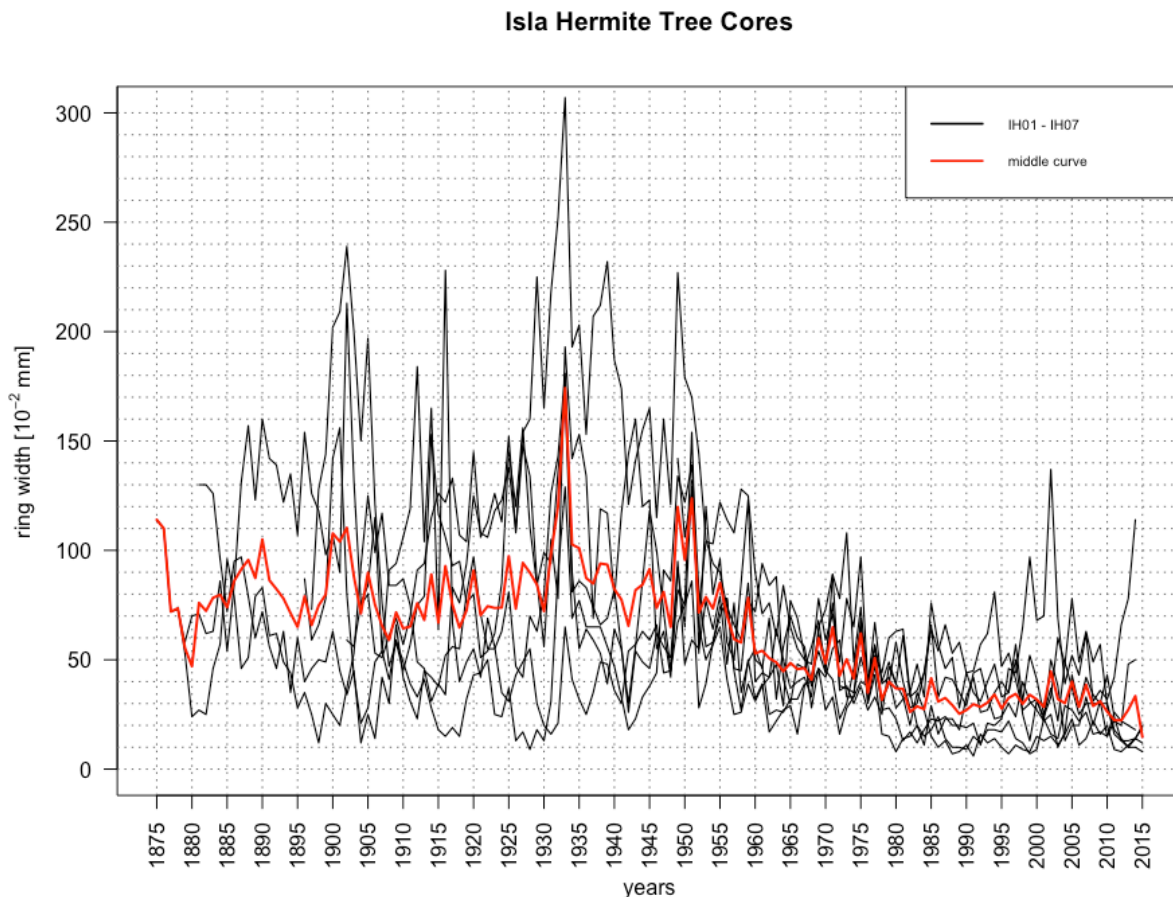
Figure 21: Overview of the measured tree-ring widths of the samples IH01-IH07 and their middle curve.

In general, the tree-ring widths of the Isla Hermite tree cores are comparably small, disregarding a few outliers. The narrowest tree ring has a width of 80 μm, whereas the broadest ring measures 3.07 mm. The tree ring of 1933 is broadly pronounced in almost all samples and was mainly used as a reference to cross date the individual tree cores within this sample size. There are periods of more narrow rings and periods of broader rings. Since 1955 the middle curve indicates a decreasing trend in the tree-ring widths. The average age of these trees amounts to 117.7 years (see Table 1). To not overrate decreasing tree-ring widths with a trees' lifetime, a tree-ring series should be corrected for the age trend with a detrending approach. The age trend describes more narrow tree rings, formed by the tree with an advancing age as the same amount of biomass is yearly created over a larger surface area due to an increasing tree radius.

Table 1: Overview of the determined ages of the tree core samples IH01-IH07.

Sample	First tree ring	Last tree ring	Age [y]
IH01	1881	2015	134
IH02	1949	2015	66
IH03	1878	2015	137
IH04	1875	2015	140
IH05	1896	2014	118
IH06	1902	2014	112
IH07	1897	2014	117
Ø **Average age:** 117.7 years			

For the detrending of this tree-ring series a 30-years spline method was applied (Bunn, 2008). The detrended series is shown in Figure 22 and the detrended individual tree cores samples can be seen in the appendix (see 10.2 Tree-ring width measurements of the samples.
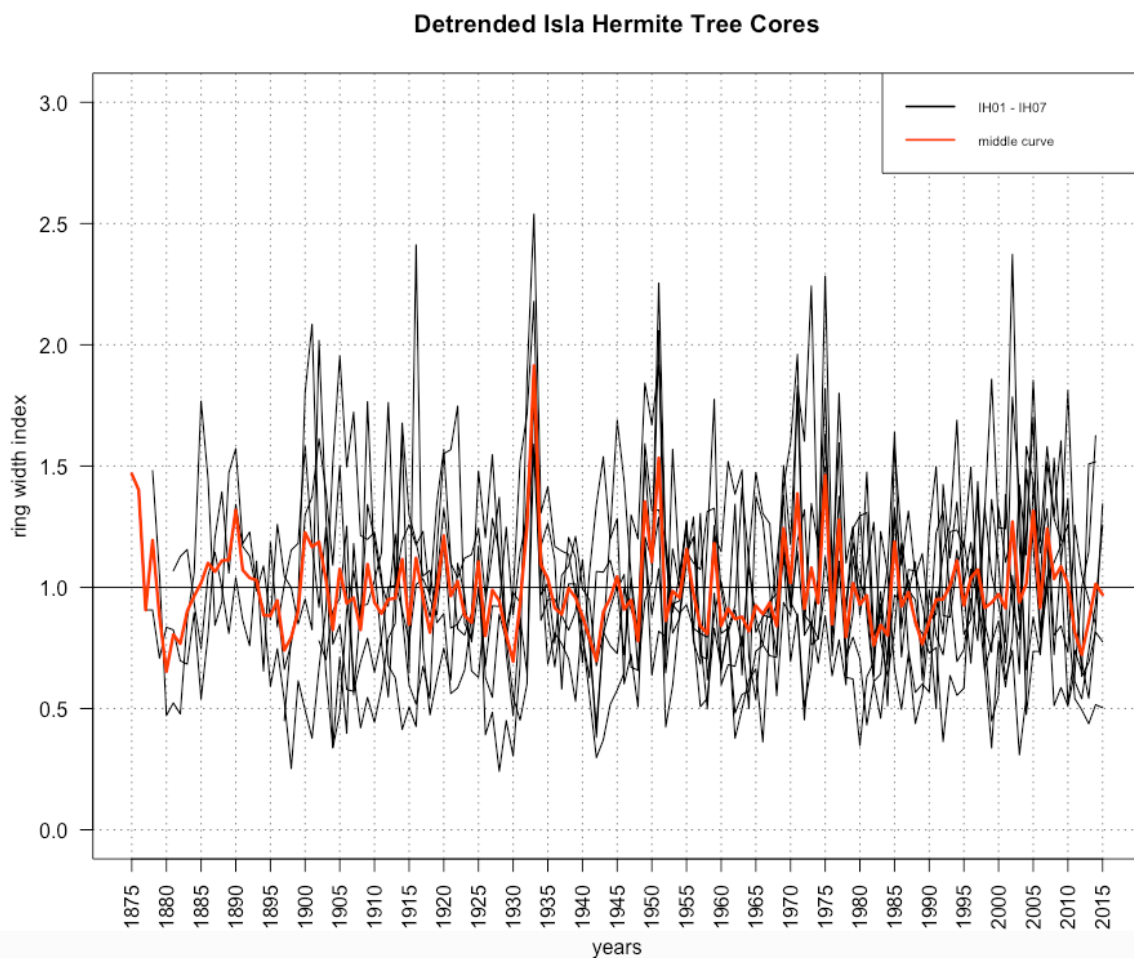
Figure 22: Overview of the detrended tree-ring width series of the samples IH01-IH07 and their middle curve.

6.2 Chemical analysis

6.2.1 Direct method: Laser ablation

The chemical composition of the four tree cores (IH01, IH03, IH04, IH05) was analyzed using laser ablation with focus on the sea salts main components sodium and chloride (see Figure 23 and 24).
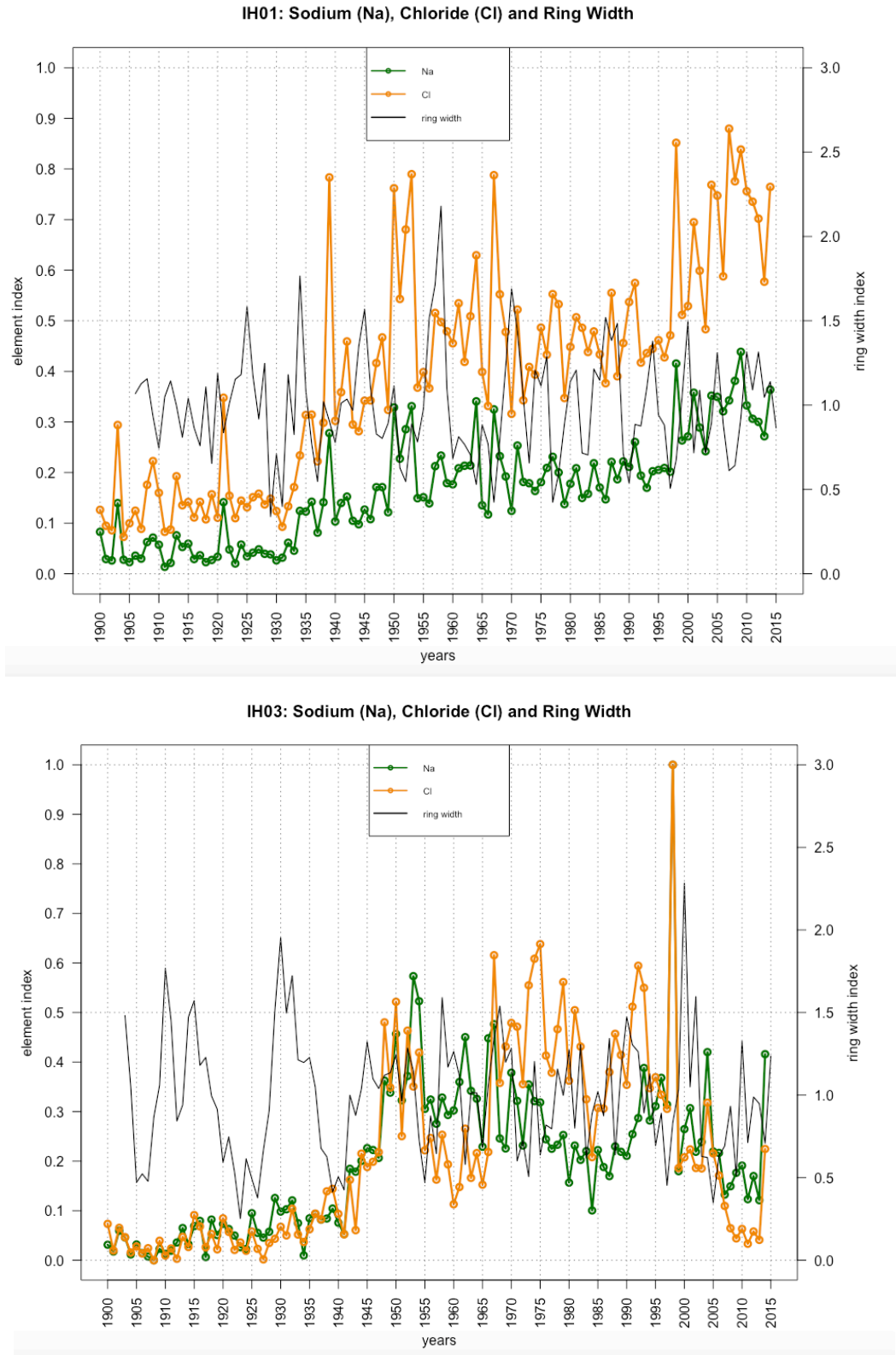
Figure 23: Detected sodium (Na), chloride (Cl) and detrended tree-ring width for samples IH01 and IH03.

IH04: Sodium (Na), Chloride (Cl) and Ring Width

IH05: Sodium (Na), Chloride (Cl) and Ring Width
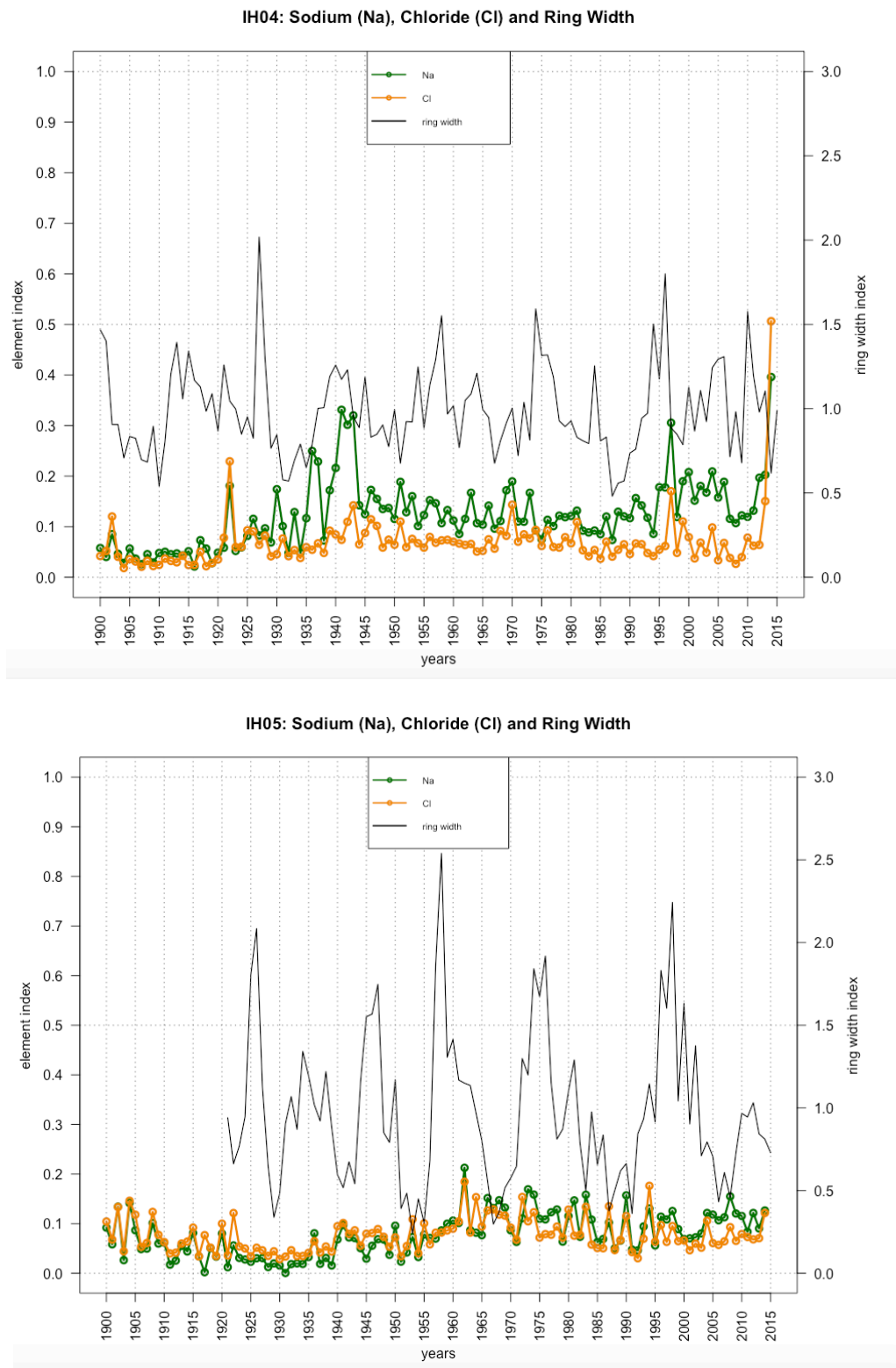
Figure 24: Detected sodium (Na), chloride (Cl) and detrended tree-ring width for samples IH04 and IH05.

In all samples, the sodium (Na) and chloride (Cl) signals behave similarly. In all samples there is an increase in sodium and chloride visible over the years. The samples IH04 and IH05 show only a slight increase, whereas IH01 and IH03 have a greater increase since the years between 1940 and 1950. For both, this general increasing trend is characterized by short term fluctuations. Other minor sea salt relevant components could also be detected in the tree cores (see 10.3 Laser ablation measurements).

6.2.2 Indirect method: Isotope analysis

The chemical composition of the six tree cores (IH01, IH03, IH04, IH05, IH06, IH07) was indirectly analyzed by investigating their oxygen and carbon stable isotopes. The measurement of the oxygen isotopes together with their tree-ring width is illustrated in Figure 25 and 26.
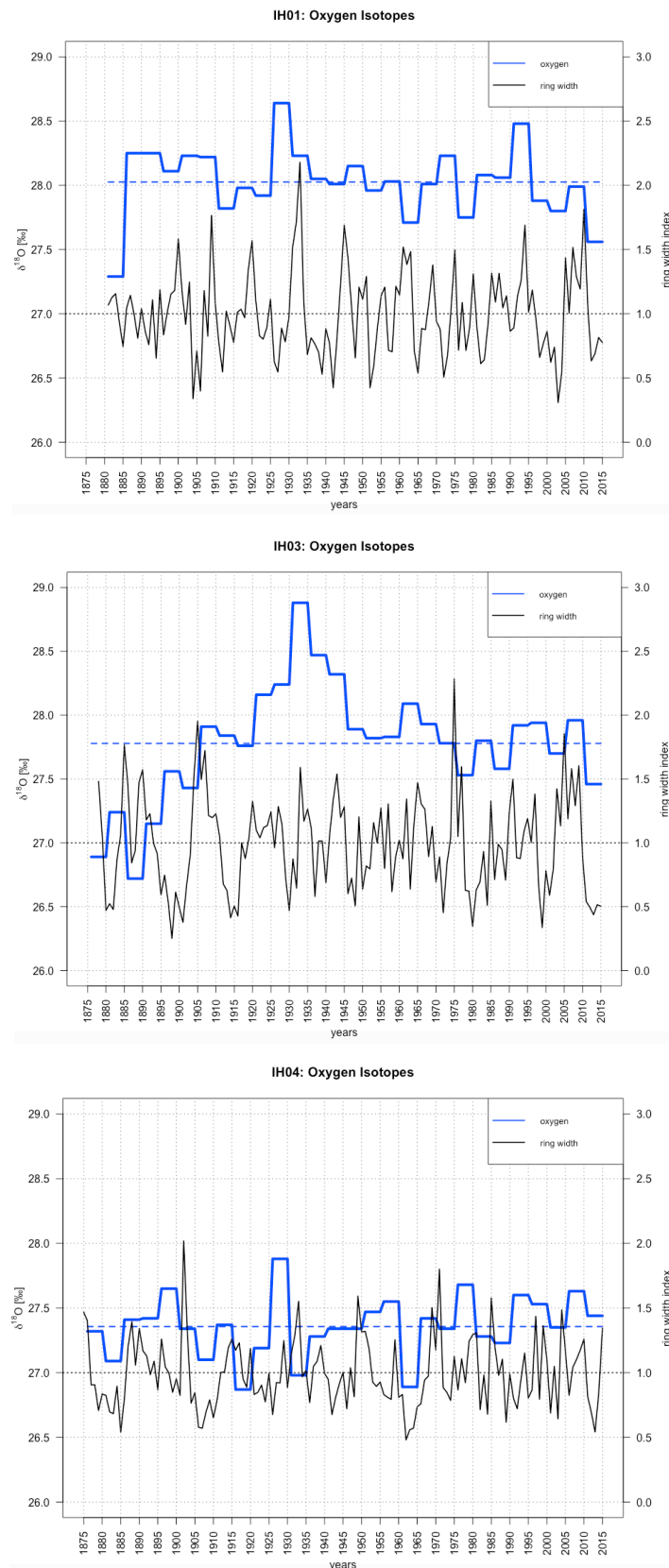
Figure 25: Oxygen isotopes with the individual mean (dashed) and the detrend ring width for samples IH01, IH03 and IH04.
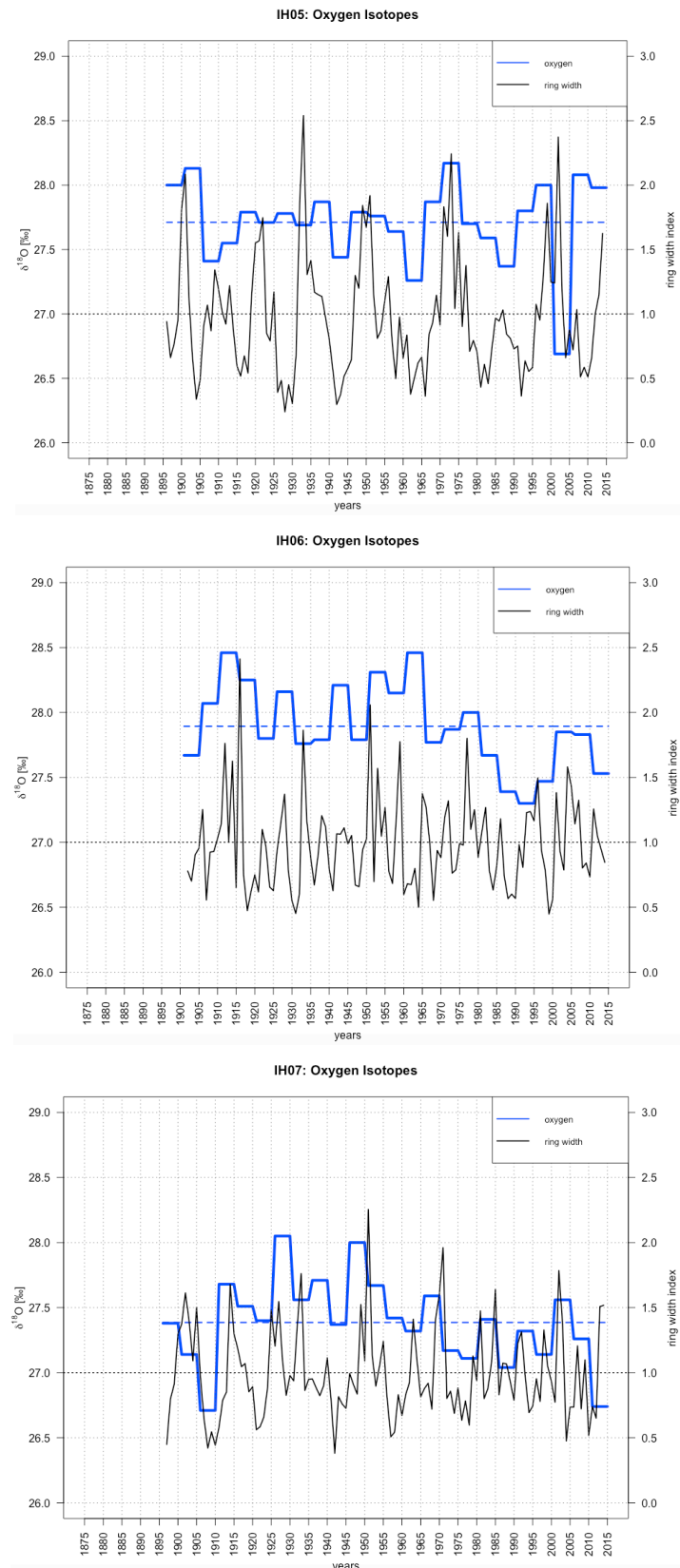
Figure 26: Oxygen isotopes with the individual mean (dashed) and the detrend ring width for samples IH05, IH06 and IH07.

Overall the oxygen isotopes in the samples do not show a general pattern or a trend over the years. In some samples (IH01, IH05) there is a short-term increase respectively decrease in the δ^{18}O value. Generally, the oxygen curves are characterized by large fluctuations of the δ^{18}O signal compared to their individual mean signal over the years.

The measurement of the carbon isotopes together with their tree-ring width is illustrated in Figure 27 and 28. For the carbon isotopes, the Suess-effect which describes the atmospheric change in heavy carbon isotopes attributed to the burning of fossil fuels was corrected for (Francey et al., 1999).
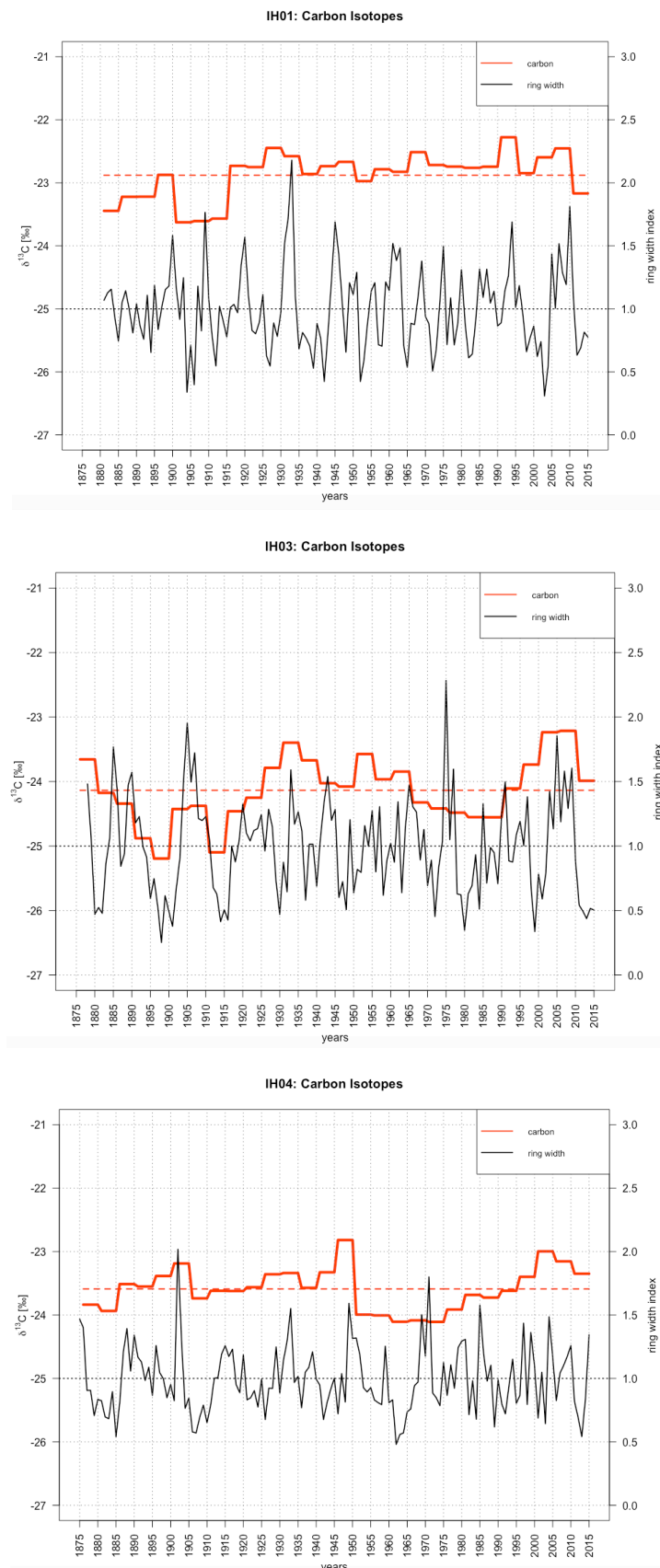
Figure 27: Carbon isotopes with the individual mean (dashed) and the detrend ring width for samples IH01, IH03 and IH04.
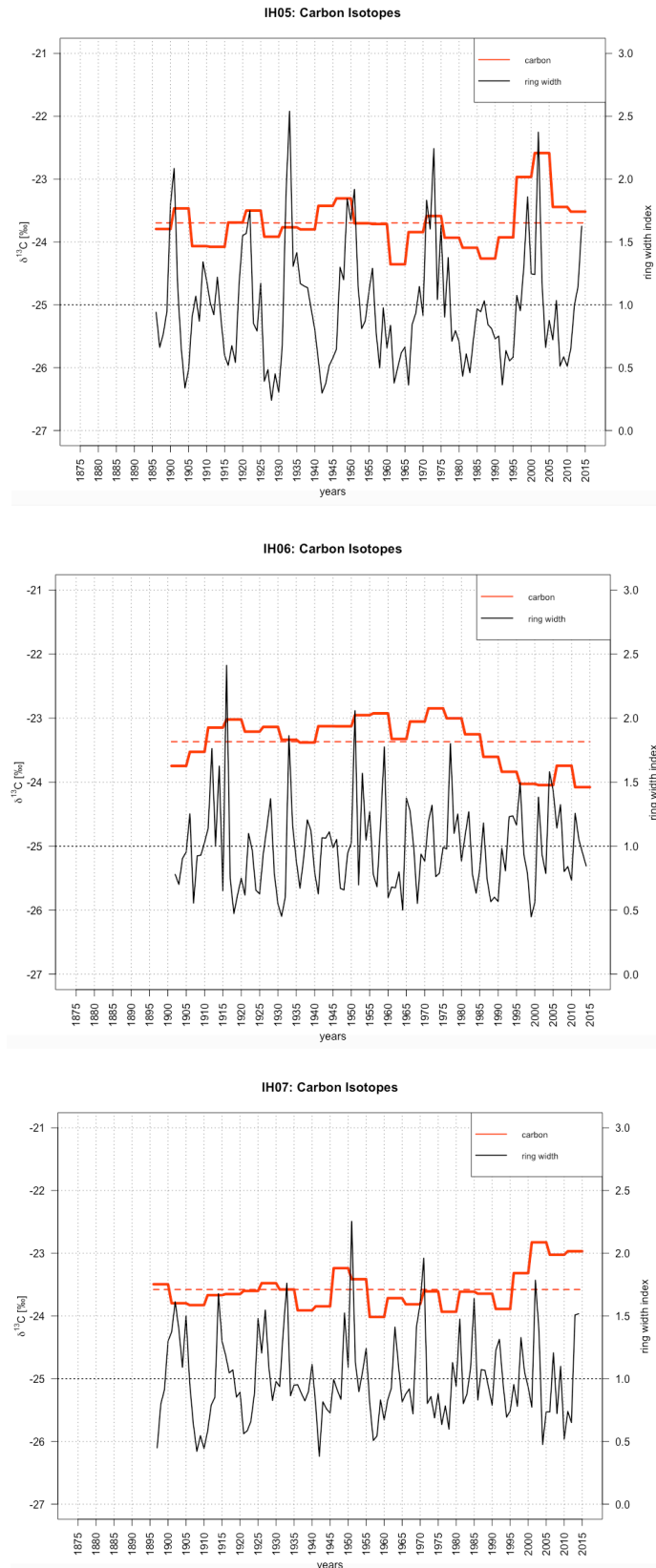
Figure 28: Carbon isotopes with the individual mean (dashed) and the detrend ring width for samples IH05, IH06 and IH07.

Overall the carbon isotopes present only small fluctuations of the δ^{13}C signal in comparison to the individual mean signal. There are no short-term changes in the δ^{13}C value. More recently around 1995, five of six samples show an increasing signal respetively less negative δ^{13}C values.

For a better understanding, the oxygen isotopes of all samples are depicted in a single figure together with their isotope middle curve and the middle tree-ring width (see Figure 29).
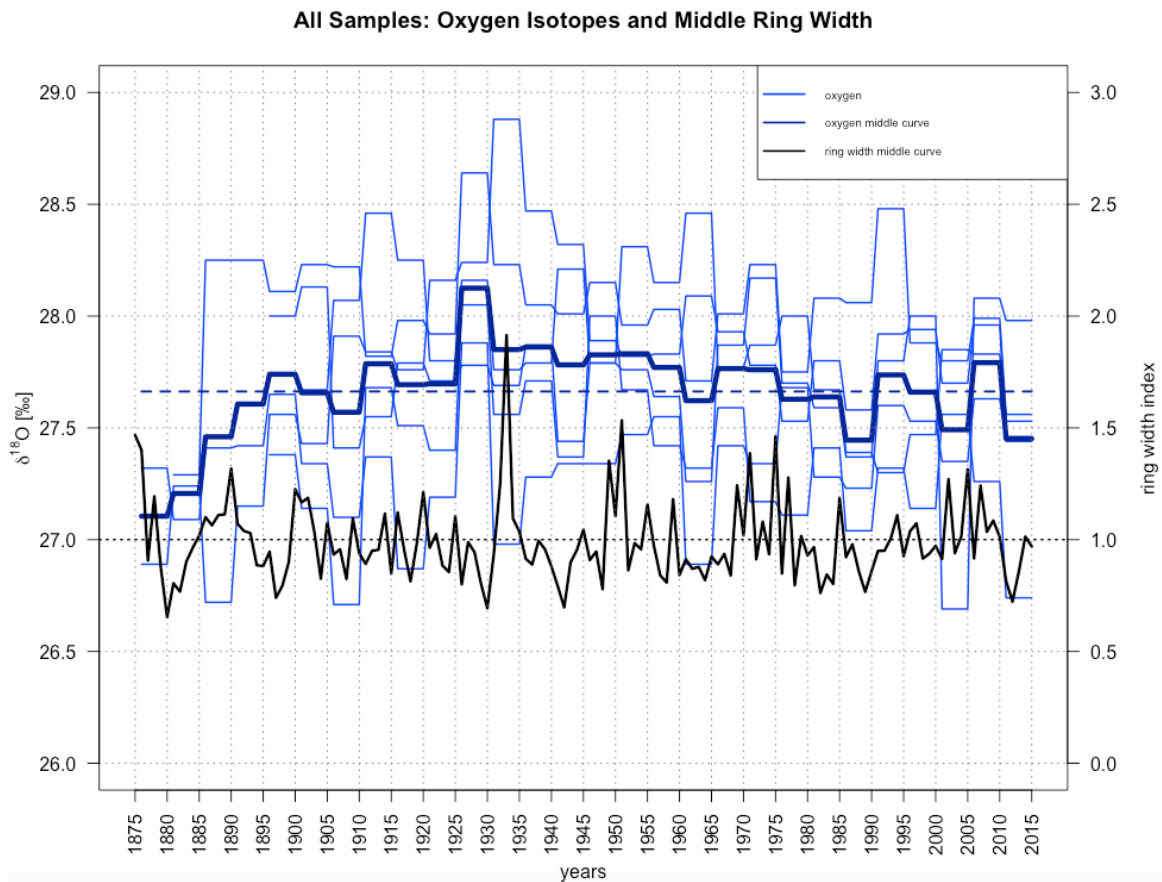
Figure 29: All tree core samples with the measured oxygen isotopes, their middle curve, the mean signal (dashed) and the detrended middle tree-ring width.

The oxygen isotopes of the different samples show a noisy signal as there is no clear pattern or trend visible over the years. Only in the beginning there is a general small increase and from 1925-1930 a short-term increase compared to the mean signal. Overall, the $\delta^{18}O$ signal of the different samples is characterized by a big heterogeneity. Further, the carbon isotopes of all samples are depicted in a single figure together with their isotope middle curve and the middle tree-ring width for a better understanding (see Figure 30).

All Samples: Carbon Isotopes and Middle Ring Width
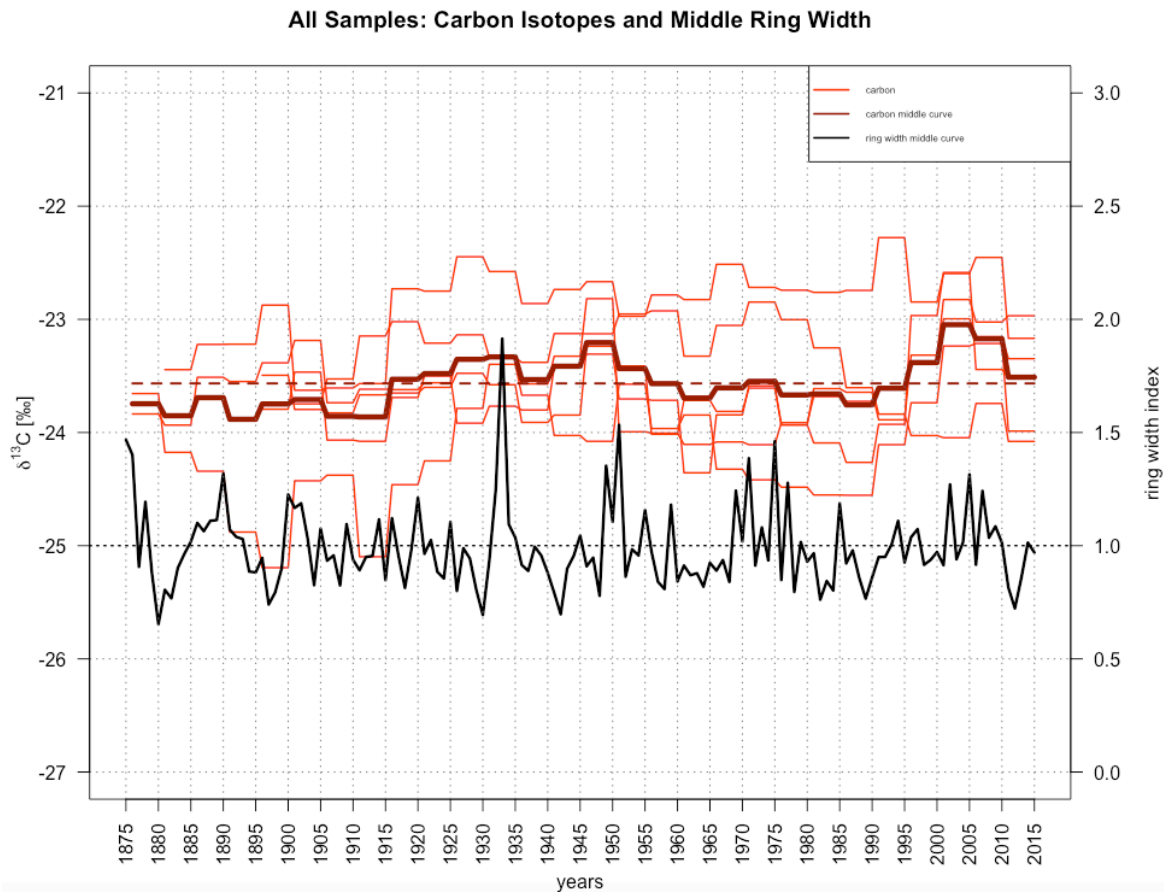
Figure 30: All tree core samples with the measured carbon isotopes, their middle curve, the mean signal (dashed) and the detrended middle tree-ring width.

The carbon isotope signal shows a comparable pattern for the different samples over the years. The individual $\delta^{13}C$ signals do not vary much from each other and it is characterized by a small overall heterogeneity. Since 1995, the increase respectively the less negative $\delta^{13}C$ values are noticeable.

6.3 The analytical methods and wind relevant data

The direct and indirect analytical methods can be compared with the SAM index, wind speed measurements from Ushuaia and reanalyzed wind speed measurements from Isla Hermite (see Figure 31).
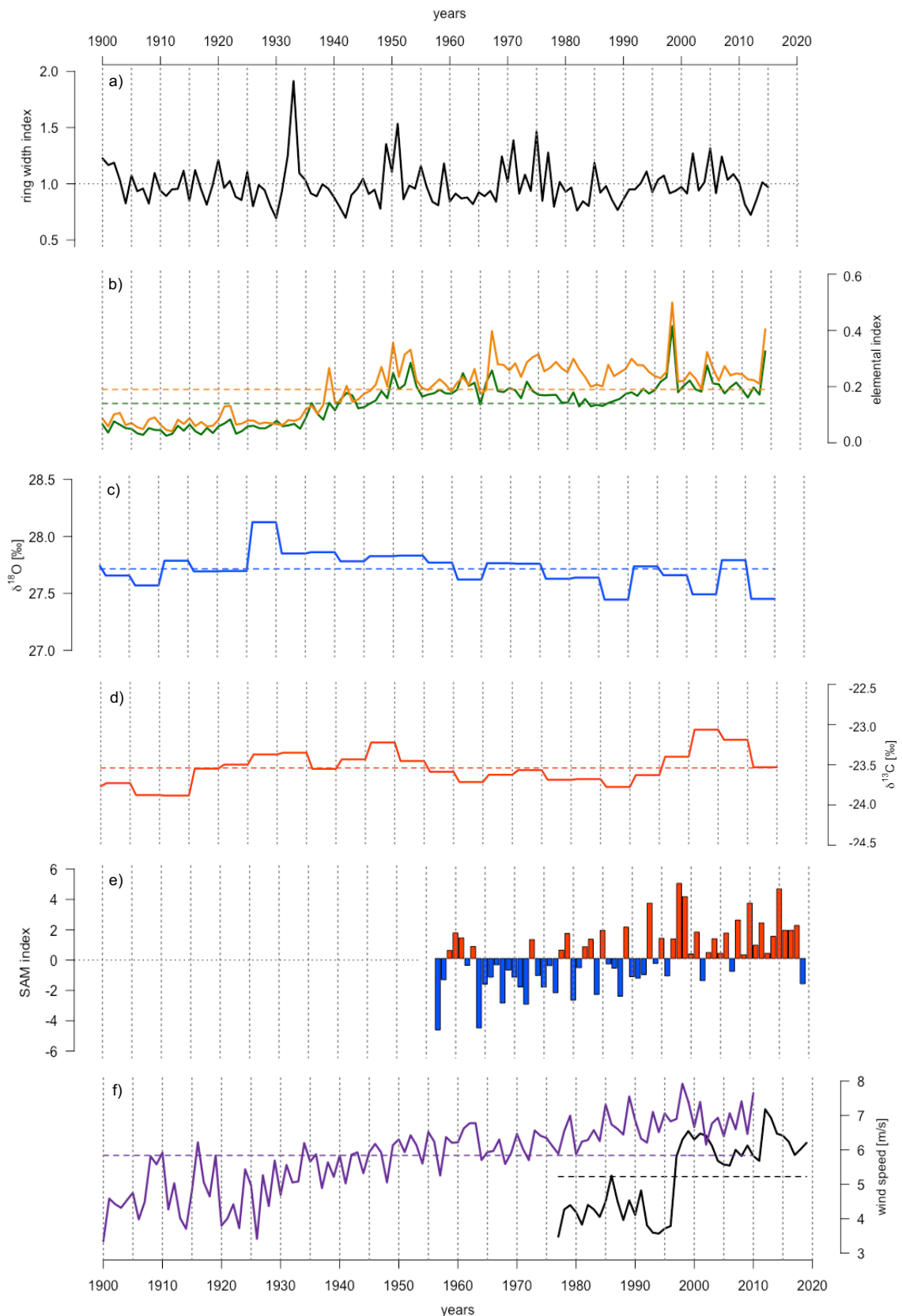
Figure 31: Comparison of the results from the direct laser ablation and indirect isotope analysis of the Isla Hermite tree cores with wind relevant data: a) middle tree-ring width of the cores b) middle Na (green) and Cl (orange) signal of the tree cores c) middle oxygen and d) carbon isotopes of the tree cores e) SAM-index, where positive values imply stronger westerlies (red) and negative values weaker westerlies (blue) (Data source: Marshall, 2003) and f) wind speed measurements of Ushuaia (black) and reanalysis of zonal wind speed measurements around Isla Hermite (purple) (Data source: BAS, personal communication; KNMI, 2020). For each curve the dashed line is the mean of that record over the time interval shown.

Graphically, the analytical methods with the sodium/chloride signal and the carbon isotopes have simi-larities with the SAM index and both wind speed measurements. Especially between 1995 and 2000 an increase respectively a clear peak can be identified in all the above-mentioned data curves. The tree-ring width and the oxygen isotopes approach do not show patterns comparable to the wind relevant data. Aside from a visual evaluation, the results of the analytical methods can be quantitively com-pared with the SAM index (see Figure 32) and the wind speed measurements (see Figure 33 and 34).
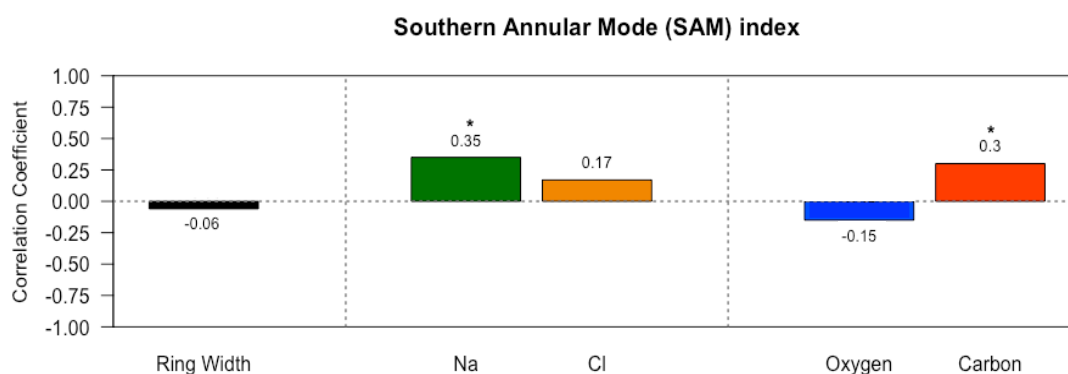
Figure 32: Pearson correlation coefficients between the applied analytical methods (Na/Cl, oxygen/carbon isotopes) and the SAM index. Significant moderate correlation is marked with *, significant good correlation with ** and significant high correlation with ***. The significance level is $\alpha < 0.05$.
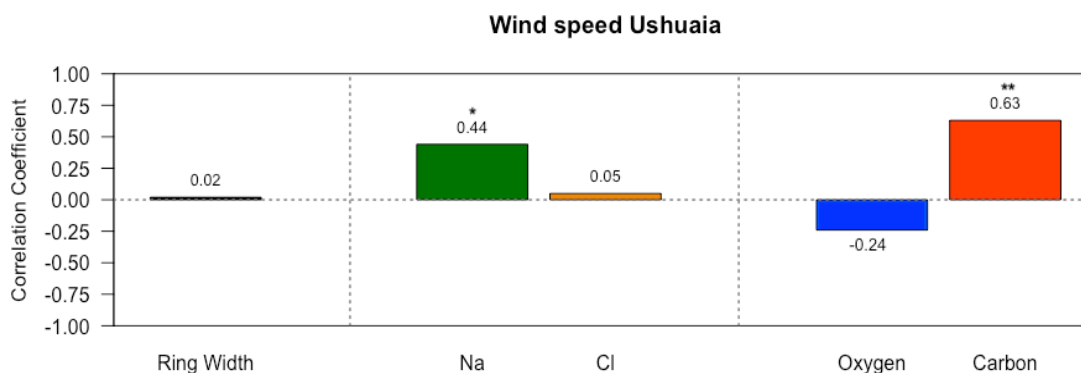
Figure 33: Pearson correlation coefficients between the applied analytical methods (Na/Cl, oxygen/carbon isotopes) and wind speed measurements from the BAS weather station in Ushuaia. Significant moderate correlation is marked with *, significant good correla-tion with ** and significant high correlation with ***. The significance level is $\alpha < 0.05$.
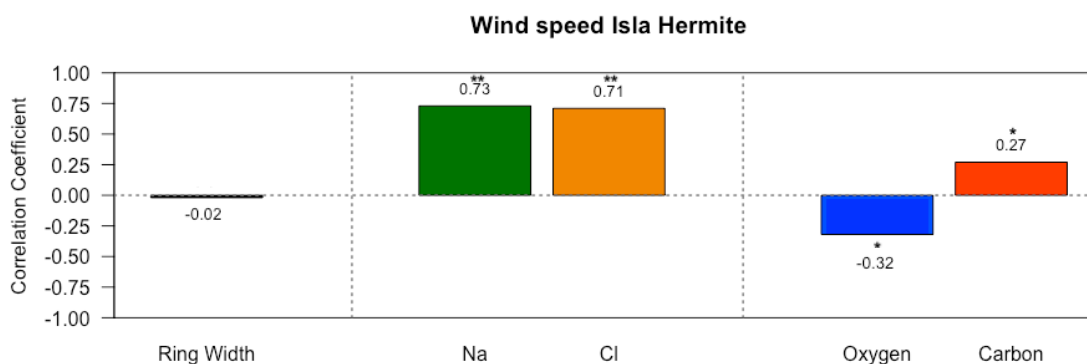
Figure 34: Pearson correlation coefficients between the applied analytical methods (Na/Cl, oxygen/carbon isotopes) and reanalysis wind speed measurements around Isla Hermite. Significant moderate correlation is marked with *, significant good correlation with ** and significant high correlation with ***. The significance level is $\alpha < 0.05$.

The highest correlations of the analytical methods with the wind relevant data exist for the reanalysis wind speed measurements around Isla Hermite. Especially the sodium (Na) and chloride (Cl) signal show good positive correlations (r = 0.73 respectively r = 0.71). A moderate positive correlation exists for the carbon isotopes and a moderate negative correlation for the oxygen isotopes. The wind speed measurements from Ushuaia significantly correlate with the carbon isotopes (r = 0.63). The sodium (Na) signal further shows a moderate positive correlation. There are no significant correlations for the chloride (Cl) signal and the oxygen isotopes. Evaluating the correlations for the SAM index, a positive moderate correlation can be found for the sodium (Na) signal and the carbon isotopes. No significant correlations exist for the chloride (Cl) signal and the oxygen isotopes. The tree-ring width presents no significant correlations with any of the wind relevant data. See the scatterplots in the appendix for more detailed information about the individual correlations of the direct and indirect methods with the wind relevant data (see 10.3 Correlations with wind relevant data and other SWW reconstructions).

6.4 Tree-ring based SWW reconstruction and other reconstructions

The results of tree-rings based reconstruction of the Southern westerly winds can be further compared with an ice core based reconstruction, where coarse particles were studied (see Figure 35).
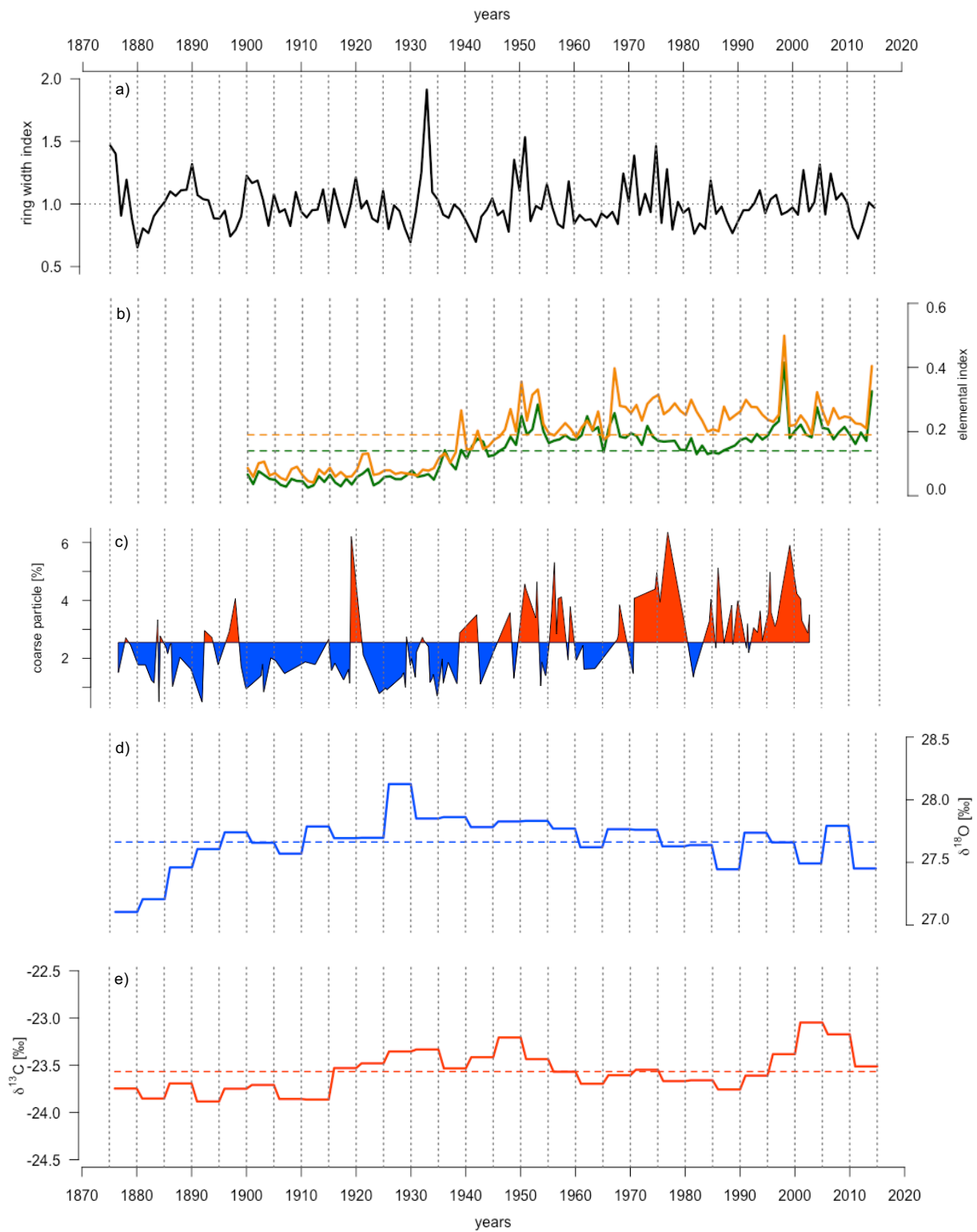
Figure 35: Comparison of the Isla Hermite tree cores based Southern westerly winds' reconstruction approaches with another SWW reconstruction method: a) middle tree-ring width of the cores b) middle Na (green) and Cl (orange) signal of the tree cores c) Ice core based SWW reconstruction with percentage of coarse particles, where more coarse particles imply stronger westerlies (red) and less coarse particles weaker westerlies (blue) (Data source: Koffman et al., 2014) d) middle oxygen and e) carbon isotopes of the tree cores. For each curve the dashed line is the mean of that record over the time interval shown.

Visually, the curves of the sodium (Na) and chloride (Cl) signal behave very similarly to the ice core record. In both records the beginning (1900-1935) is characterized by a low signal with one exception around 1920. The elements of sodium (Na) and chloride (Cl) show an increase around 1922/1923 and the ice cores present a pronounced peak in 1919. The next 20 years (1920-1940) is in both records dominated by a continuous low signal. Subsequently, both records show high signals with comparable peaks, notably in 1940, 1947, 1951 and 1953. Lower signals then reappear between 1955-1970 in both records. During this period, the ice core record reveals some increases what the sodium (Na) and chloride (Cl) signals do not explicitly show. Nevertheless, both show an increase of their signal around 1966/67. These high signals continue during the next decade (1970-1980), before dropping notably in 1982 for the ice cores and in 1985 for the sodium (Na) and chloride (Cl) signals. The end of both records is mainly characterized by a high signal and a pronounced peak can be observed around 1998 for both. The isotopes-based reconstruction approaches show in general less similarities with the ice core-based reconstruction. The carbon isotopes show a continuous increase since 1990 with a peak signal for 2000-2005. This behavior is comparable with the high signal of the ice cores during this time. The low signal period of the ice core record (1870-1920) can also be observed in the carbon isotopes (1870-1915). For the oxygen isotopes no similar patterns can be found. The oxygen isotopes show a pronounced peak for the time between 1925-1930 and could be comparable to the ice core record peak of 1919. In the past 25 years, where the carbon isotopes and the ice core record show an increase, the oxygen isotopes reveal an opposite behavior with a general low signal. Aside from this visual comparison, the direct and indirect methods of a tree-ring based Southern westerly winds reconstruction can be quantitatively compared to the ice core based SWW reconstruction (see Figure 36)
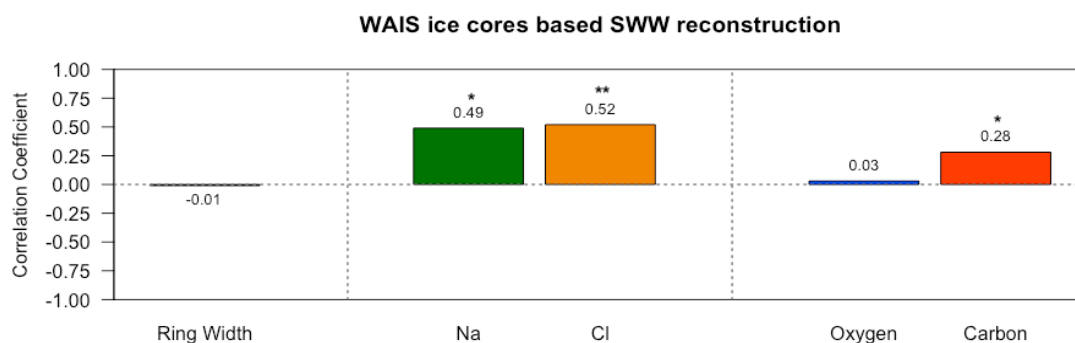
Figure 36: Pearson correlation coefficients between tree-ring based SWW reconstructions (Na/Cl, oxygen/carbon isotopes) and the West Antarctic Ice Sheet (WAIS) ice cores based SWW reconstruction. Significant moderate correlation is marked with *, significant good correlation with ** and significant high correlation with ***. The significance level is $\alpha < 0.05$.

The direct reconstruction method with the sodium (Na) and chloride (Cl) signal shows the strongest correlation with the ice core-based reconstruction ($r = 0.49$ and $r = 0.52$). A moderate positive correlation exists for the indirect reconstruction method with the carbon isotopes. There are no significant correlations for the tree-ring width and the oxygen isotopes. For further information about the correlations of the direct and indirect methods of reconstructing the Southern westerly winds with the ice core-based reconstruction see the scatterplots in the appendix (see 10.3 Correlations with wind relevant data and other SWW reconstructions).

7   Discussion

7.1   Tree-ring width measurement

The results of the ring width measurements show that the Isla Hermite trees generally have narrow tree-ring widths with some broadly pronounced years. After the correction for the age trend, the detrended series presents no unusual growth patterns with the exception of some broad tree rings (1933, 1951, 1975) and some narrow tree rings (1930, 1942, 2012). Considering that these trees grow in an extreme climate of low temperatures, resulting in a short growing period, the narrow tree rings are reasonable. Temperature and precipitation are the main factors that influence the growth of the tree rings. The lack of meteorological long-term records across this remote region complicates the evaluation of the observed growth behavior. A temperature reconstruction from the area of Ushuaia and Tierra del Fuego Island exists (Boninsegna et al. 2009). Nevertheless, no reasonable explanations can be made for the observed growth patterns of the Isla Hermite trees based on the existing temperature record. To further check the plausibility of the Isla Hermite tree-ring series, it can be set in contrast to rarely existing tree-rings chronologies from this area. There is a 200-years chronology of *Nothofagus betuloides* trees on Navarino Island (Lombardi et al., 2011) and of *Nothofagus pumilio* trees from eastern Tierra del Fuego Island in Argentina (Matskovsky et al., 2019). When the *Nothofagus antarctica* trees-based series from Isla Hermite is put in contrast to these two chronologies, no obvious comparable growth patterns can be elaborated. TOn a bigger spatial scale, two studies showed no major disruption of tree growth patterns in southern Chile, or even a recent lower tree growth in the Patagonian area (Innes et al., 2000; Villalba et al., 2012). These observations also apply to the Isla Hermite tree-ring series as no major disruption in the tree -ring growth can be identified. A recent low tree growth can also hold true for the Isla Hermite trees, but longer measurements of this study site are missing to fully support and prove this observation. To sum up, the above-mentioned comparisons and considerations about the tree ring series of Isla Hermite support the existing observation, that based on the strong geographical and climatic heterogeneity in this whole region, environmental or ecological factors at the microsite level are supposed to have a bigger influence on the tree-ring growth (Fuentes et al., 2019).

7.2   Analytical methods for wind relevant data

7.2.1   Direct method: Laser ablation

The laser ablation measurements demonstrate that in all examined tree cores a sodium (Na) and chloride (Cl) signal could be detected with an increase in the signal over the years. Half of the samples show only a slight increase and the other half presents a great increase since around 1940/1950 with short term decreases and increases. As sodium (Na) and chloride (Cl) behaves very similar in the samples, these elements can be assumed to be present as the composited sodium chloride (NaCl), which is the major component of sea salt. Other sea salt relevant elements such as magnesium, calcium and potassium could also be detected in the tree rings and show comparable behaviors to the two major components (see 10.3 Laser ablation measurements).

As all the above-mentioned elements naturally occur in many living organisms, basic amounts of some elements can also be found in trees (Vaganov et al., 2013). The detected sodium (Na) and chloride (Cl) signals in the trees cannot be conclusively led back to sea water, unless measurements of wood control samples for this trees' species from this region are conducted with no direct wind and ocean influence. However, the suggested relation is that the detected intensities of sodium (Na) and chloride (Cl) in the tree rings mirror the behavior of the winds. Stronger westerly winds lead to enhanced transport and uptake of sea salt components by the trees. On the contrary, the transport and uptake of the sea salt components is decreased with weaker westerlies. The leaves and roots seem both possible ways for the uptake of this signal. In other studies, enhanced chloride concentrations could be detected in trees that took chloride up mainly through the roots from a chloride-enriched wetland or sodium and chloride cations could be determined in cotton leaves that were exposed to simulated salt dust (Yanosky and Kappel, 1997; Abuduwaili et al., 2015). Another study showed that in plants the transport of liquid water or solutes from aerosols across activated stomata can occur as an adaption process of nutrient uptake in nutrient poor soils (Burkhardt, 2010). Transferred to the Isla Hermite trees, wind-driven sea salt components are possibly taken up by the trees through the stomata from deposition on their leaves. The other possibility is that the winds deposit sea salt components on the ground and the trees then take up soil- or groundwater diluted with sea salt through their roots. A study revealed that silver nanoparticles entered the tree stem faster through the leaves than through the roots (Cocozza et al., 2019). The penetration of the bark as way of sea salt components entering the Isla Hermite trees appears unlikely. The westerly winds are strong but for an uptake through the bark, extensive mechanical pressure would be needed. In another study only increased concentrations of airborne particles were incorporated in the bark of trees and not in the tree rings (Chiarantini et al., 2016).

In conclusion, increasing sodium (Na) and chloride (Cl) signals, which are main components of sea salt could be detected in the tree rings. A mechanism that westerly winds transport sea salt relevant components, which are taken up by the trees and archived in their rings, appears reasonable. An uptake of the signal seems possible through the roots or the stomata of the leaves. The detected sodium (Na) and chloride (Cl) signals in the tree rings are likely to yield wind relevant data.

7.2.2 Indirect method: Isotope analysis

The results of the isotope analysis reveal that the measured oxygen isotopes in the different tree core samples show a noisy $\delta^{18}O$ signal with a big heterogeneity and no clear patterns or trends over the years. The heterogenous oxygen signal can be explained by the fact that the $\delta^{18}O$ signal in tree rings is controlled by the stomatal conductance but mainly resembles the isotopic oxygen signal of the source water, taken up by the trees. It makes a difference for a tree whether its water uptake stems from precipitation, from the seawater or the soil water. Generally, sea water has a $\delta^{18}O$ signal around 0‰, soil water around -3‰ to -10‰ and precipitation around -5‰ to -20‰ dependent on the geographical location (Van Meerveld, 2019). The existing isotopic signal of the water source influences the $\delta^{18}O$ signal in the tree rings. Therefore, the isotopic oxygen signal mainly resembles the source water and

the westerly winds play only a limited or no role in a trees' water uptake process. The winds indirectly influence the precipitation patterns as they can direct saturated clouds with rainfall over the island and to the trees. The lack of precipitation measurements for this remote location of Isla Hermite, complicates the identification of wind spatiotemporal patterns. However, it is important to remember that on these islands, the microclimate (e.g. windward or leeward side of small mountains) plays likely the dominant role and influences how much rainfall is deposited.

In the area of southernmost South America, a $\delta^{18}O$ tree-ring chronology from the foothills of the northwestern Patagonian Andes in Argentina exists (Roig et al., 2006). The Argentinean chronology presents a noisy $\delta^{18}O$ signal with a different course over the years and denotes a mean signal of $\delta^{18}O$ = 24‰ compared to $\delta^{18}O$ = 27.7‰ of this study. A verification of the results of this study based on a comparison with the Argentinean chronology is difficult as the locations are different. The $\delta^{18}O$ signal of deposited rainfall is generally influenced by the Latitude-, Elevation- and Continental effect. With an increase of these effects, the $\delta^{18}O$ value of the deposited rainfall water decreases (Van Meerveld, 2019). The averaged $\delta^{18}O$ precipitation signal for the Argentinean and the Isla Hermite study site is for both around -10‰ (Araguás-Araguás et al., 2000). However, the lower mean $\delta^{18}O$ signal in the Andean foothill trees can be attributed to the rainwater that is more enriched with the lighter oxygen isotopes (low $\delta^{18}O$ signal) when these particluar trees mainly take up rainwater. As the clouds have already moved over the Andes, they mostly rained out, resulting in lower $\delta^{18}O$ higher values in the rainwater and subsequently in the tree rings.

To sum up, the oxygen isotope signal in trees is mainly influencd by the water source and the role of the winds in the water uptake process is only minor. The winds influence precipitation patterns by directing saturated clouds over islands, but the isoptic oxygen signal of rainfall is further dependent on other factors which include the Latitude-, Elevation- or Continental effect. Long term meteological data from this remote island is required to make reliable statements about precipitation spatiotemporal patterns and to understand the minor role of winds on the oxygen signal in trees. The oxygen isotopes in the Isla Hermite trees yield no wind relevant data.

On the other hand, the measured carbon isotopes show small $\delta^{13}C$ fluctuations in the different tree core samples over the observed time span with a recent trend of less negative $\delta^{13}C$ values. The carbon isotopes in tree rings are influenced by the rates of stomatal conductance and photosynthesis (McCarroll and Loader, 2014). The indirect role of winds on these physiological processes is still disputed and not fully understood. Higher wind speeds are argued to induce greater transpiration rates that lead to a greater water stress for a tree. As a consequence, the trees' stomata are closed and the tree rings are enriched with the heavier carbon isotopes, leading to less negative $\delta^{13}C$ values (Bidwell, 1979). The observed trend of the less negative $\delta^{13}C$ values in the Isla Hermite tree cores during 1995-2005 could therefore indicate stronger winds: The westerly winds strengthened, enhanced transpiration rates followed, which led to a water stress for the trees resulting in closing of their stomata. Winds are also supposed to have a more mechanical influence on the stomata: In response to the physical shock of wind, the stomata may shut, or stomatal damage is caused (Caldwell, 1970; Wilson, 1979). Damaged

stomata lead to greater water loss, which is aimed to be reduced by the tree with the closure of the stomata. As a result, the heavier carbon isotope is enriched, leading to less negative $\delta^{13}C$ values. Conversely, the shock of wind is also proposed to open the stomata even more widely which results in more negative $\delta^{13}C$ values (Grace, 1974). Another explanation for less negative $\delta^{13}C$ values could be wind-driven salt that constitutes a further stress factor for the tree. It could be shown that salt respectively root immersion in saltwater caused higher $\delta^{13}C$ values in tree rings which were likely triggered by the osmotic stress from saltwater (Kubota et al., 2017). Therefore, stronger winds could bring more sea salt, causing an additional stress factor for the tree and prompts a further closure of the stomata.

In summary, the general role of winds on the carbon isotopes in trees is yet not fully clear but the explanations of closed or damaged stomata, due to water and salt stress from stronger westerly winds seem plausible. The carbon isotopes in trees possibly yield some wind relevant data.

7.2.3 Application of the direct and indirect method

Aside from yielding wind relevant data, the application of the direct laser ablation and the indirect isotopes analysis can be compared. Laser ablation is a non-destructive approach that allows to measure a range of elements in tree rings with a high spatial resolution. The method is simple to apply with the corresponding instruments, but exclusive and expensive instruments are needed. A limit of laser shots is available per measuring run, that allows only a few tree cores to be simultaneously measured. Given that the method is able to measure in the μm range, it is highly suitable for narrow tree rings like the examined Isla Hermite tree cores. Laser ablation constitutes a new approach in dendrochronology with yet only little data for comparisons. On the other hand, the indirect method of isotope analysis is a well-known and established approach in dendrochronology. It is a destructive approach that enables to measure changes in the per mill range of oxygen and carbon isotopes in tree rings. A high-resolution can be achieved as year to year changes are examined by splitting single tree rings. A yearly splitting was mechanically not possible with the Isla Hermite samples since the individual rings were too narrow. The sample preparation for the isotope analysis is time consuming and the measurements are costly. A lot of data about isotopes in trees is available and the mechanisms are known, but the role of winds on isotopes in trees is not fully understood.

7.3 Comparison of wind signal from tree-ring record with meteorological data

Figure 31 and the corresponding correlation analysis show that some analytical methods, namely the sodium (Na) and chloride (Cl) signal and the carbon isotopes, present good similarities with wind relevant regional meteorological records. The highest correlations (r = 0.73 and r = 0.71) could be elaborated for the sodium (Na) and chloride (Cl) signal with the wind speed measurements from Isla Hermite. These elements also present good correlations with wind speed measurements from Ushuaia and the SAM index, suggesting stronger winds go along with higher intensities of sodium (Na) and chloride (Cl) in the tree rings. It is likely that these detected signals in the Isla Hermite trees are induced by the westerly winds. The assumed underlying mechanism of stirred up sea-salt that is transported onto

the island by the winds and is then taken up by the trees seems reasonable, as sodium (Na) and chloride (Cl) constitute the main components of sea salt. This apparent direct connection between the element signals and the wind speed measurements, makes it more likely that sodium (Na) and chloride (Cl) is taken up by the trees through the stomata of the leaves. An indirect way over the roots from sea salt diluted rain- or soil water appears less likely as in this case a more diffuse signal would be expected. Stronger westerly winds lead to enhanced transport and uptake of sea salt components by the trees and consequently results in higher intensities of the elements in the tree rings. It is likely, that the detected odium (Na) and chloride (Cl) signals in the tree rings constitute a wind relevant signal.

Furthermore, the carbon isotopes show good correlations with wind speed measurements from Ushuaia (r = 0.63) and moderate correlations with the Isla Hermite wind speed measurements and the SAM index. Especially the peaks of SAM and the increases in wind speed during the period of 1995-2000 appears to be retrieved in the oxygen isotopes with a trend of less negative $\delta^{13}C$ values during the same period. When the Isla Hermite wind speed measurements indicate weaker westerly winds from around 2005, the carbon isotopes show more negative $\delta^{13}C$ values. At the same time, the exact role of the winds on the carbon isotopes in trees and the underlying mechanisms are yet to be established. Nonetheless, the explanations of closed or damaged stomata through water and salt stress induced by stronger winds seem plausible. A wind relevant signal in the carbon isotopes of tree rings is possible. In contrast, the oxygen isotopes show only low negative correlations with wind relevant data. The role of winds on the oxygen isotopes in tree rings can be denoted as minor as other factors including the type of water source, the geographical effects on precipitation seem to be more prominent. A wind relevant signal in the oxygen isotopes of tree rings is unlikely based on the Isla Hermite trees.

The tree-ring width shows no significant correlations with the wind relevant data. The winds appear to have no significant influence on the growth of the tree rings. The constantly blowing westerly winds constitute probably more a long-lasting constraint and the trees are very likely accustomed to these strong windy conditions. For the trees, the winds do not constitute a sudden extreme event that could more likely be visible as disturbed growth behaviour in the tree rings. A wind induced signal in the growth of the tree rings cannot be observed. Overall, a wind relevant signal can be retrieved from the Isla Hermite tree cores as some approaches show good correlations with wind relevant regional meteorological data. Retrieving a wind relevant signal is likely from detected sodium (Na) and chloride (Cl) signals and potentially also from the carbon isotopes in tree rings. No wind relevant signal can be derived from the oxygen isotopes in tree rings and from the tree-ring width.

7.4 Comparison of the tree-ring based SWW reconstruction with other reconstructions

Figure 35 and the corresponding correlation analysis demonstrates that some tree-ring based SWW reconstruction approaches, namely the sodium (Na), chloride (Cl) signal and the carbon isotopes present some close similarities to the ice core based SWW reconstruction. The highest correlations (r = 0.49 and r = 0.52) could be reached for the sodium (Na) and chloride (Cl) signal approach. As these

signals already show the best correlations with wind relevant data, it makes sense that they are also best capable of reconstructing the behavior of westerly winds. The timing of the peaks of the signals that signify stronger westerlies, fits well with the peaks of the coarse particles in the ice-core based approach. Although the peaks are well depicted in the two records, a shift of the peaks around two to three years can sometimes be identified. Lows in the chemical signals, which correspond to weaker westerlies, are less pronounced compared to the ice-core based reconstruction. An explanation could be that in tree rings already a basic amount of naturally occurring sodium (Na) and chloride (Cl) exists which cannot be even more negative in times of weaker westerlies. Consequently, no such pronounced low signals can be developed in this record. In contrast, the ice cores make use of a different approach as strong and weak westerlies are determined based on the coarse particles' sizes in the ice cores. In addition, the tree-ring based method does not yet have longer records which would allow to build a more robust long-term mean based on which low and high signals can be clearer distinguished.

The carbon isotope based SWW reconstruction presents some similarities with the ice core-based reconstruction. It depicts an analogous period of a low carbon signal with weak westerlies during 1870-1915 and a recent carbon signals' increase with stronger westerlies from 1995. Apart from that, the carbon isotope approach is not able to reconstruct the short-term dynamics of the westerlies since it is also based on five year means and not on annual values. As previously mentioned in the discussion with wind relevant data, the role of winds on carbon isotopes in tree rings and the underlying mechanism are not fully understood. This aggravates the use of carbon isotopes to reconstruct the westerlies based on an only indirect approach. Besides this, the approach of using the oxygen isotopes in tree rings or the tree-ring width are not able to reconstruct the Southern westerly winds. This makes sense since they presented no significant correlations with wind relevant data.

Aside from this ice core based SWW reconstruction, more approaches, focused on the more recent behaviour, are lacking for a quantitative comparison. Nevertheless, this tree-ring based SWW reconstruction can be qualitatively compared with approaches focusing more on the whole Holocene. For instance, the iron concentration in marine sediments, biogenic carbonate accumulation rates in lake sediments or the type of pollen records were used (Lamy et al., 2001; Lamy et al., 2010; Strother et al., 2015). Such proxy records allow to reconstruct the Southern westerly winds over a link with a climate variable (e.g. precipitation, temperature) and the modern relationship between the climate variable and the winds. In contrast to these more conventional approaches, a tree-ring based reconstruction has an annual resolution, as one specific signal can be assigned to an exact year respectively an annual ring of the tree. The focus lies more on the recent wind behavior and the decadal changes with possible implications for the future climate system. The detected sodium (Na) or chloride (Cl) signals directly reflect the behavior respectively the strength of the westerlies and is not indirectly derived over a climate variable. Unfavourable is that this tree-ring based reconstruction is not able to cover the suggested 250-year periodicity of the westerlies since the examined trees are on average 118 years old (Turney et al., 2016). The uptake mechanism behind the reconstruction approach of a wind induced sea salt signal which is taken up by the trees appears reasonable but could not yet been conclusively proven. The

proxy of tree respectively its occurrence is limited in such high latitudes within the core wind belt due to the prevailing extreme climate.

Finally, the tree-ring based method using sodium (Na) and chloride (Cl) signals, correlates well with an ice core based SWW reconstruction. It presents some advantages compared to the conventional reconstruction methods, but also several disadvantages, which can be improved with further work and research. Altogether, it constitutes a promising alternative approach to reconstruct the Southern westerly winds with a focus on their recent behaviour and decadal changes for future climate implications.

7.5   Future trends of the Southern westerly winds in the climate system

The applied methods within this thesis confirm the observed strengthening trend of the Southern westerly winds in recent decades. Sodium (Na), chloride (Cl) and carbon isotopes show increasing signals over the observed years with a recent stronger increase from around 1995. They provide signs that there could also be a recent short-term weakening of the westerlies within the long-term intensification trend. The wind speed measurements from Ushuaia support this speculation. At this point, it cannot be confidently stated whether this is only a short-term decrease in the long-term westerlies' intensification trend or not, but the long-term strengthening trend is apparent.

The underlying mechanisms for the recent strengthening and southward shift of the westerlies are still controversially debated. It is not clear whether the southward shift and strengthening is a response to elevated carbon dioxide in the atmosphere or intensified westerlies themselves cause an increase of atmospheric carbon dioxide (Toggweiler, 2009). The solar irradiance is proposed to modulate the westerlies in the long-term and the recent shift and the intensification is also attributed to stratospheric ozone depletion in the Antarctic region with a smaller effect of greenhouse gas forcing (Turney et al., 2016; Lee and Feldstein, 2013). In the past, shifted and strengthened westerlies are suggested to have substantially increased the ventilation of carbon-rich deep water in the Southern Ocean at the end of the last Ice Age and triggered CO_2-induced warming (Anderson et al., 2009). Given the strong link between the Southern westerly winds and the Southern Ocean, where enormous quantities of carbon are stored and heat is taken up, further research about the exact underlying mechanism and resulting consequences are essential. It is decisive whether the expected intensification of the westerlies, leading to enhanced carbon-rich deep-water upwelling, will transform the Southern Ocean from a current carbon sink into a carbon source or whether an enhanced upwelling can be covered by the Southern Ocean with a more extensive carbon uptake. In times of a rapidly changing climate and increasing atmospheric carbon dioxide, we learn that the westerlies will probably be more intensified and play a central role how the future climate looks given they interplay with the Southern Ocean in the global carbon cycle. Lastly, we can learn that more research about the westerly winds is extremely helpful to better estimate future consequences in the global climate system.

8   Conclusion

A better understanding of the Southern westerly winds, which are a major driver of the global climate is crucial to assess future consequences in our climate system. This thesis indicates that the applied methods of chemical analysis, namely laser ablation and carbon isotope analysis allow to retrieve a wind relevant signal in tree rings from southernmost South America. Laser ablated sodium (Na) and chloride (Cl) signals in the tree rings present strong positive correlations with regional wind speed measurements (r = 0.73 and r = 0.71). The detection and existing correlations of these main components of sea salt support the idea that the Isla Hermite trees are likely to take up sea salt components induced by the westerly winds. An uptake of the trees appears possible through their leaves or roots. The apparent direct connection between the detected element's signals and the wind speed measurements makes it more likely that sea salt components are taken up through the stomata of their leaves compared to the roots with an expected more diffuse and long-term signal. Higher intensities of sodium (Na) and chloride (Cl) in the tree rings signify stronger westerly winds as more sea salt is transported by the winds and taken up by the trees. Besides this, the carbon isotope analysis correlates moderately with wind speed measurements and possibly constitutes a wind relevant signal. The exact role of winds on carbon isotopes in trees with the underlying mechanisms are not yet fully understood. Closed or damaged stomata, due to water and salt stress from stronger winds seem plausible.

The findings of these approaches demonstrate the potential of a tree-ring based reconstruction of the Southern westerly winds. It creates interesting possibilities to develop a high-resolved reconstruction of the Southern westerly winds with a focus on their recent behavior and decadal to centennial-scale shifts with future implications for the climate. A SWW reconstruction based on the laser ablated sodium (Na) and chloride (Cl) signals in the tree rings correlates significantly with an ice core based SWW reconstruction (r = 0.49 and r = 0.52). The non-destructive method of laser ablation is characterized by high spatial and temporal resolution for narrow rings and is simple to apply with the required instruments. A SWW reconstruction using carbon isotope analysis is less promising as only moderate correlations could be found. The method has a lower temporal resolution, is more time consuming and the winds' role on carbon isotopes in trees yet more unclear.

In the future, more work is required to improve this approach and to further exploit the existing potential of a tree-ring based SWW reconstruction. Sampling of more tree cores from this remote region would be highly beneficial to verify these results, improve the spatial representation and build more robust tree-ring series. The availability of living trees in such high latitudes is limited. A future sampling approach could be more systematic in terms of the location of the trees and taking necessary control samples, including the leaves of the trees. Open questions could be conclusively answered about the prevailing way of sodium (Na) and chloride (Cl) uptake by the trees, the detailed influence of the winds on the trees and possible wind induced damages of the stomata. This thesis showed that dendrochronology with a chemical analysis of tree rings can help to better understand the Southern westerly winds by investigating sodium (Na) and chloride (Cl) signals in the tree rings.

9 References

Abuduwaili J., Zhaoyong Z., Feng Qing J. & Dong Wei L. (2015): The disastrous effects of salt dust deposition on cotton leaf photosynthesis and the cell physiological properties in the Ebinur Basin in Northwest China. *PLoS ONE 10*(5), p.1-24.

Anderson R. F., Ali S., Bradtmiller L. I., Nielsen S. H. H., Fleisher M. Q., Anderson B. E. & Burckle L. H. (2009): Wind-Driven Upwelling in the Southern Ocean and the Deglacial Rise in Atmospheric CO_2. *Science 323*, p. 1443-1448.

Araguás-Araguás L., Froehlich K. & Rozanski K. (2000): Deuterium and oxygen-18 isotope composition of precipitation and atmospheric moisture. *Hydrological processes 14*(8), p. 1341-1355.

Australis (2017): Website Australis Cape Horn & Patagonia. Kap Horn: Karte und Geschichte dieser legendären Landspitze. Available: https://blogpatagonien.australis.com/kap-hoorn-karte-und-geschichte-dieser-legendaren-landspitze/ [Accessed: 21.08.20]

BAS (2015): Field report Isla Hermite 2015. British Antarctic Survey (BAS). Cambridge.

Biblioteca del Congreso Nacional (2020): Official Website Library of the National Congress of Chile. Clima y vegetación Región de Magallanes. Available: https://www.bcn.cl/siit/nuestropais/region12/clima.htm [Accessed: 21.04.20]

Bidwell R. C. S. (1979): Plant physiology. Second edition. Macmillan: New York.

Blum W. E. (1974): Salzaufnahme durch die Wurzeln und ihre Auswirkungen. *European Journal of Forest Pathology 4(1),* p. 41-44.

Boninsegna J. A., Argollo J., Aravena J. C., Barichivich J., Christie D., Ferrero M. E., Lara A., Le Quesne C., Luckman B. H., Masiokas M., Morales M., Oliveira J. M., Roig F., Srur A. and Villalba R. (2009): Dendroclimatological reconstructions in South America: A review. *Palaeogeography, Palaeoclimatology, Palaeoecology 281(3-4),* p. 210-228.

Bunn A. G. (2008): A dendrochronology program library in R (dplR). *Dendrochronologia 26(2),* p. 115-124.

Burkhardt J. (2010): Hygroscopic particles on leaves: nutrients or desiccants? *Ecological Monographs 80(3),* p. 369-399.

Caldwell M. M. (1970): Plant gas exchange at high wind speeds. *Plant Physiology 46(4),* p. 535-537.

Chiarantini L., Rimond V., Benvenuti M., Beutel M. W., Costagliola P., Gonnelli C., Lattanzi P. & Paolieri M. (2016): Black pine (Pinus nigra) barks as biomonitors of airborne mercury pollution. *Science of the Total Environment 569*, p. 105-113.

Cocozza C., Perone A., Giordano C., Salvatici M. C., Pignatelli S., Raio A., Schaub M., Sever K., Innes J. L., Tognetti R. & Cherubini P. (2019): Silver nanoparticles enter the tree stem faster through leaves than through roots. *Tree Physiology 39(7),* p. 1251-1261.

Coutts M. P. and Grace J. (Eds.) (1995): Wind and trees. Cambridge University Press: Cambridge, New York, Melbourne.

D'Arrigo R. D. and Villalba R. (2000): Review of dendroclimatic research at high latitudes in South America: Indicators of atmosphere-ocean climate variability. In Roig F. A. (comp.). *Dendrocronología en América Latina*. EDIUNC: Mendoza, Argentina, p. 271-282.

Dixon M. and Grace J. (1984): Effect of wind on the transpiration of young trees. *Annals of Botany 53(6)*, p. 811-819.

Douglass A. E. (1941): Crossdating in Dendrochronology. *Journal of Forestry 39(10),* p. 825-831.

EEA (2012): Particulate matter from natural sources and related reporting under the EU Air Quality Directive in 2008 and 2009. European Environment Agency (EEA) technical report. Chapter 3, Sea salt aerosols. Luxembourg: Publications Office of the European Union, p. 19-20.

Encyclopedia Britannica (2019): Website of the Encyclopedia Britannica. Meteorology. Westerlies. Available: https://www.britannica.com/science/westerlies [Accessed: 02.11.19]

Fernández B., Claverie F., Pécheyran C. & Donard O. F. X. (2007): Direct analysis of solid samples by fs-LA-ICP-MS. *Trends in Analytical Chemistry 26(10),* p. 951-966.

Francey R. J., Allison C. E., Etheridge D. M., Trudinger C. M., Enting I. G., Leuenberger M., Langenfelds R. L., Michel E. & Steele L. P. (1999): A 1000-year high precision record of $\delta^{13}C$ in atmospheric CO_2, *Tellus Series B Chemical and Physical Meteorology 51(2),* p. 170-193.

Frölicher T. L., Sarmiento J. L., Paynter D. J., Dunne J. P., Krasting J. P. & Winton M. (2015): Dominance of the Southern Ocean in Anthropogenic Carbon and Heat Uptake in CMIP5 Models. *Journal of Climate 28(2),* p. 862–86.

Fuentes M., Aravena J. C., Seim A. & Linderholm H. W. (2019): Assessing the dendroclimatic potential of Nothofagus betuloides (Magellan's beech) forests in the southernmost Chilean Patagonia. *Trees 33(2),* p. 557-575.

Gärtner H. and Nievergelt D. (2010): The core-microtome: A new tool for surface preparation on cores and time series analysis of varying cell parameters. *Dendrochronologia 28(2),* p.85-92.

Gillett N. P., Zwiers F. W., Weaver A. J. & Stott P. A. (2003): Detection of human influence on sea-level pressure. *Nature 422,* p. 292-294.

Grace J. (1974): The effect of wind on grasses: 1. cuticular and stomatal transpiration. *Journal of Experimental Botany 25(3),* p. 542-551.

Gray J. and Thompson P. (1977): Climatic information from 18 O/16 O analysis of cellulose, lignin and whole wood from tree rings. *Nature 270*, p. 708-709.

Guillong M., Meier D. L., Allan M. M., Heinrich C. A. & Yardley B. W. D. (2008): Sills: a MATLAB-based program for the reduction of Laser Ablation ICP-MS data of homogeneous materials and inclusions. *Mineralogical Association of Canada Short Course 40*, Vancouver, B.C., p. 328-333.

Hertzberg J. (2017): Ice-sheet history revealed by fossils. *Nature 547*, p. 35–36.

Heusser C. J. (1989): Late Quaternary Vegetation and Climate of Southern Tierra del Fuego. *Quaternary Research 31(3),* p. 396-406.

Hillenbrand C. D., Smith J. A., Hodell D. A., Greaves M., Poole C. R., Kender S., Williams M., Andersen T. J., Jernas P. E., Elderfield H., Klages J. P. Roberts S. J., Gohl K., Larter R. D. & Kuhn G. (2017): West Antarctic Ice Sheet retreat driven by Holocene warm water incursions. *Nature 547*, p. 43–48.

Hoad S. P., Jeffree C. E., & Grace J. (1992): Effects of wind and abrasion on cuticular integrity in Fagus sylvatica L. and consequences for transfer of pollutants through leaf surfaces. *Agriculture, Ecosystems and environment 42(3-4)*, p. 275-289.

Hodgson D. A. and Sime L. C. (2010): Paleoclimate: Southern westerlies and CO_2. *Nature Geoscience 3*, p. 666-667.

Holland P. R., Bracegirdle T. J., Dutrieux P., Jenkins A. & Steig E. J. (2019): West Antarctic ice loss influenced by internal climate variability and anthropogenic forcing. *Nature Geoscience 12(9),* p. 718–24.

Innes J. L., Schneiter G., Waldner P. & Bräker O. U. (2000): Latitudinal variations in tree growth in southern Chile. In Roig F. A. (comp.). *Dendrocronología en América Latina*. EDIUNC: Mendoza, Argentina, p. 177-192.

Jones B. (2020): Webiste University of Oxford. Oxford Plants 400. Plant 154. Nothofagus antarctica. Available: https://herbaria.plants.ox.ac.uk/bol/plants400/Profiles/MN/Nothofagus [Accessed: 22.04.20]

Kaennel M. and Schweingruber F. H. (1995): Multilingual Glossary of Dendrochronology. Terms and Definitions in English, German, French, Spanish, Italian, Portuguese, and Russian. Birmensdorf, Swiss Federal Institute for Forest, Snow and Landscape Research. Haupt: Berne, Stuttgart, Vienna.

References

Kilian R. and Lamy F. (2012): A review of Glacial and Holocene paleoclimate records from southernmost Patagonia (49-55°S). *Quaternary Science Reviews 53*, p. 1–23.

KNMI (2020): Website of the Royal Dutch Meteorological Institute. Climate Explorer. Available: http://climexp.knmi.nl/select.cgi?field=era20c_u10m>climexp.knmi.nl/select.cgi?field=era20c_u 10m[Accessed: 17.04.20]

Koffman B. G., Kreutz K. J., Breton D. J., Kane E. J., Winski D. A., Birkel S. D., Kurbatov A. V. & Handley M. J. (2014): Centennial-scale variability of the Southern Hemisphere westerly wind belt in the eastern Pacific over the past two millennia. *Climate of the Past 10(3)*, p. 1125-1144.

Kubota T., Kagawa A. & Kodama N. (2017): Effects of salt water immersion caused by a tsunami on $\delta^{13}C$ and $\delta^{18}O$ values of Pinus thunbergii tree-ring cellulose. *Ecological research 32(2)*, p. 271-277.

Lamy F., Hebbeln D., Röhl U. & Wefer G. (2001): Holocene rainfall variability in southern Chile: a marine record of latitudinal shifts of the Southern Westerlies. *Earth and Planetary Science Letters 185(3-4)*, p. 369–382.

Lamy F., Kaiser J., Arz H. W., Hebbeln D., Ninnemann U., Timm O., Timmermann A. & Toggweiler J. R. (2007): Modulation of the bipolar seesaw in the Southeast Pacific during Termination 1. *Earth and Planetary Science Letter*s 259*(3-4),* p. 400-413.

Lamy F., Kilian R., Arz H. W, Francois J. P., Kaiser J., Prange M. & Steinke T. (2010): Holocene changes in the position and intensity of the southern westerly wind belt. *Nature Geoscience 3 (10),* p. 695–699.

Le Quéré C., Rödenbeck C, Buitenhuis E. T., Conway T. J., Langenfelds R., Gomez A., Labuschagne C., Ramonet M., Nakazawa T., Metzl N., Gillett N. & Heimann M. (2007): Saturation of the southern ocean CO2 sink due to recent climate change. *Science 316,* p. 1735–38.

Lee S. and Feldstein S. B. (2013): Detecting ozone-and greenhouse gas–driven wind trends with observational data. *Science 339(6119),* p. 563-567.

Liu Y., Ta W., Cherubini P., Liu R., Wang Y. & Sun C. (2018): Elements content in tree rings from Xi'an, China and environmental variations in the past 30 years. *Science of the Total Environment 619*, p. 120-126.

Loader N. J., McCarroll D., Barker S., Jalkanen R. & Grudd H. (2017): Inter-annual carbon isotope analysis of tree-rings by laser ablation. *Chemical Geology 466*, p. 323–26.

Lombardi F., Cocozza C., Lasserre B., Tognetti R. & Marchetti M. (2011): Dendrochronological assessment of the time since death of dead wood in an old growth Magellan's beech forest, Navarino Island (Chile). *Austral Ecology 36*(3), p. 329-340.

Marshall G. J. (2003): Trends in the Southern Annular Mode from observations and reanalyses. *Journal of Climate 16(24),* p. 4134–4143.

Martin J. A. R., Gutiérrez C., Torrijos M. & Nanos N. (2018): Wood and bark of Pinus halepensis as archives of heavy metal pollution in the Mediterranean Region. *Environmental pollution 239,* p. 438-447.

Matskovsky V., Roig F. A. & Pastur G. M. (2019): Removal of a non-climatically induced seven-year cycle from Nothofagus pumilio tree-ring width chronologies from Tierra del Fuego, Argentina for their use in climate reconstructions. *Dendrochronologia 57*, p.1-9.

McCarroll D. and Loader N. J. (2004): Stable isotopes in tree rings. *Quaternary Science Reviews 23(7-8),* p. 771-801.

Millero F. J., Feistel R., Wright D. G. & McDougall T. J. (2008): The composition of Standard Seawater and the definition of the Reference-Composition Salinity Scale. *Deep Sea Research Part I: Oceanographic Research Papers 55(1),* p. 50-72.

Moy C. M., Seltzer G. O., Rodbell D. T. & Anderson D. M. (2002): Variability of El Niño/Southern Oscillation activity at millennial timescales during the Holocene epoch. *Nature* 420, p. 162-165.

NASA (2009): Website of the National Aeronautics and Space Administration (NASA). Earth. Sea Salt Aerosols. Available: https://svs.gsfc.nasa.gov/10390 [Accessed: 28.04.20]

Pariona A. (2018): What Are The Westerlies? Website World Atlas. Available: https://www.worldatlas.com/articles/what-are-the-westerlies.html [Accessed: 19.03.20]

Perone A., Cocozza C., Cherubini P., Bachmann O., Guillong M., Lasserre B., Marchetti M. & Tognetti R. (2018): Oak tree-rings record spatial-temporal pollution trends from different sources in Terni (Central Italy). *Environmental Pollution 233*, p. 278-289.

Petersen A., Eckstein D. and Liese W. (1982): Holzbiologische Untersuchungen über den Einfluss von Auftausalz auf Hamburger Strassenbäume. *Forstwissenschaftliches Centralblatt 101(1)*, p. 353-365.

Ponce J. F. and Fernández M. (2014). Climatic and environmental history of Isla de los Estados, Argentina. Springer: Dordrecht, Heidelberg, New York, London.

Pruppacher H. R. and Klett J.D. (1997): Microphysics of Clouds and Precipitation. The Atmospheric Aerosol and Trace Gases, Chapter 8. Springer: Dordrecht, Netherlands, p.216-286.

Rintoul S.R., Hughes C. & Olbers D. (2001). The Antarctic Circumpolar Current System. In: Siedler G., Church J. & Gould J. (eds.). *Ocean circulation and climate; observing and modelling the global ocean.* International Geophysics Series, 77. Academic Press: San Diego, p. 271-302.

Rodrigues C., Maia R., Lauteri M., Brugnoli E. & Máguas C. (2013): Stable Isotope Analysis. Chapter 4. In: Guardia M. and Gonzálvez A. (eds.) *Food Protected Designation of Origin: Methodologies and Applications*. Comprehensive Analytical Chemistry 60. Elsevier: Oxford, p. 77-99.

Roig F. A., Siegwolf R., & Boninsegna J. A. (2006): Stable oxygen isotopes (δ 18 O) in Austrocedrus chilensis tree rings reflect climate variability in northwestern Patagonia, Argentina. *International journal of biometeorology 51(2),* p. 97-105.

Rolfo M. and Ardrizzi G. (2013): Patagonia & Tierra del Fuego. Nautical Guide. Second Edition. Cabo de Hornos. Available: http://www.capehorn-pilot.com/immagini/Charts/10.7%20Cabo%20de%20Hornos.htm [Accessed: 21.08.20]

Saunders K. M., Hodgson D. A., Mcmurtrie S. & Grosjean M. (2015): A diatom-conductivity transfer function for reconstructing past changes in the Southern Hemisphere westerly winds over the Southern Ocean. *Journal of Quaternary Science 30(5),* p. 464–477.

Saunders K. M.,. Roberts S. J, Perren B., Butz C., Sime L., Davies S., Nieuwenhuyze W. V., Grosjean M. &. Hodgson D. A. (2018): Holocene dynamics of the Southern Hemisphere westerly winds and possible links to CO2 outgassing. *Nature Geoscience 11(9),* p. 650–55.

Schimpf D., Kilian R., Kronz A., Simon K., Spötl C., Wörner G., Deininger M. & Mangini A. (2011): The significance of chemical, isotopic, and detrital components in three coeval stalagmites from the superhumid southernmost Andes (53°S) as high-resolution palaeo-climate proxies. *Quaternary Science Reviews 30(3-4),* p. 443-459.

Shindell D. T. and Schmidt G. A. (2004): Southern Hemisphere climate response to ozone changes and greenhouse gas increases. *Geophysical research letters 31(18),* p. 1-4.

Sigman D. M., Hain M. P. & Haug G. H. (2010): The polar ocean and glacial cycles in atmospheric CO_2 concentration. *Nature 466,* p. 47-55

Steinhilber F., Beer J. & Fröhlich C. (2009): Total solar irradiance during the Holocene. *Geophysical Research Letters 36(19),* p. 1-5.

Strother S. L., Salzmann U., Roberts S. J., Hodgson D. A, Woodward J., Nieuwenhuyze W. V., Verleyen E., Vyverman W., & Moreton S. G. (2015): Changes in Holocene climate and the intensity of Southern Hemisphere Westerly Winds based on a high-resolution palynological record from sub-Antarctic South Georgia. *The Holocene 25(2*), p. 263–279.

Swart N. C. and Fyfe J. C. (2012): Observed and simulated changes in the Southern Hemisphere surface westerly wind-stress. *Geophysical Research Letters 39(16*), p. 1-6.

Tofwerk AG (2017): Website Tofwerk AG, Globla leader in Mass Spectrometry. What is Laser Ablation ICP-MS Imaging? Available: https://www.tofwerk.com/laser-ablation-icp-ms-imaging/ [Accessed: 31.07.20]

Toggweiler J. R., Russell J. L. & Carson S. R. (2006): Midlatitude westerlies, atmospheric CO2, and climate change during the ice ages. *Paleoceanography 21(2),* p. 1-15.

Toggweiler J. R. (2009): Climate change. Shifting westerlies. Science *323,* p. 1434-1435.

Tomasi C. and Lupi A. (2017): Primary and Secondary Sources of Atmospheric Aerosol. In Tomasi C., Fuzzi S. and Kokhanovsky A. (eds.) *Atmospheric Aerosols: Life Cycles and Effects on Air Quality and Climate.* Weinheim, Germany: Wiley-VCH Verlag GmbH & Co. KGaA, p.1-86.

Treydte K. (2019): Stable isotopes in tree rings (δ^{13}C and δ^{18}O). Dendroecology course, Swiss Federal Institute of Technology (ETH), Zurich.

Turney C. S. M., Jones R. T., Fogwill C., Hatton J., Williams A. N., Hogg A., Thomas Z. A., Palmer J., Mooney S. & Reimer R.W. (2016): A 250-year periodicity in Southern Hemisphere westerly winds over the last 2600 years. *Climate of the Past 12*, p. 189-200.

Vaganov E. A., Grachev A. M., Shishov V. V., Panyushkina I. P., Leavitt S. W., Knorre A. A., Chebykin E. P. & Menyailo, O. V. (2013): Elemental composition of tree rings: A new perspective in Biogeochemistry. *Doklady Biological Sciences 453,* p. 375-379.

Van Meerveld I. (2019): Lecture notes Isotope application in geographical research: Isotopes in hydrological studies. Department of Geography, University of Zurich.

Veblen T. T., Donoso C., Kitzberger T. & Rebertus A. J. (1996): Ecology of southern Chilean and Argentinean Nothofagus forests. In: Veblen T. T., Hill R. S. & Read J. (eds.) *The ecology and biogeography of Nothofagus forests*. Yale University Press: New Haven and London, p. 293-353.

Villalba R., Lara A., Masiokas M. H., Urrutia R., Luckman B. H., Marshall G. J., Mundo I. A., Christie D. A., Cook E. R., Neukom R., Allen K., Fenwick P., Boninsegna J. A., Srur A. M., Morales M. S., Araneo D., Palmer J. G., Cuq E., Aravena J. C., Holz A. & LeQuesne C. (2012). Unusual Southern Hemisphere tree growth patterns induced by changes in the Southern Annular Mode. *Nature geoscience 5(11),* p. 793-798.

Vuaridel M., Cherubini P., Mettra F., Vennemann T. & Lane S. N. (2019): Climate-driven change in the water sourced by trees in a de-glaciating proglacial fore-field, Torres del Paine, Chile. *Ecohydrology 12(7),* p. 1-13.

Wikipedia (2015): Website Wikipedia The Free Encyclopedia. Hermite-Inseln. Available: https://de.wikipedia.org/wiki/Hermite-Inseln [Accessed: 15.04.20]

Wilson J. (1979): Some physiological responses of Acer pseudoplatanus L. to wind at different levels of soil water, and the anatomical features of abrasive leaf damage. Doctoral dissertation, University of Edinburgh.

Xercavins Comas, Agustín (1984): Notas sobre el clima de Magallanes (Chile). *Revista de geografía 18(1),* p. 95-110.

Yan H., Sun L., Wang Y., Huang W., Qiu S., & Yang C. (2011): A record of the Southern Oscillation Index for the past 2,000 years from precipitation proxies. *Nature Geoscience 4*, p. 611-614.

Yanosky T. M., Hupp C. R. and Hackney C. T. (1995): Chloride concentrations in growth rings of Taxodium distichum in a saltwater-intruded estuary. *Ecological Applications 5(3),* p.785-792.

Yanosky T. M. and Kappel W. M. (1997): Effects of solution mining of salt on wetland hydrology as inferred from tree rings. *Water Resources Research 33(3),* p. 457-470.

Ziska L. H., De Jong T. M., Hoffman G. F. & Mead R. M. (1991): Sodium and chloride distribution in salt-stressed Prunus salicina, a deciduous tree species. *Tree physiology 8(1),* p. 47-57.

10 Appendix

10.1 Sampling details of the BAS-expedition in 2015

Table 2: Overview of the sampling details of the tree cores IH01-IH07 during the BAS-expedition in 2015

Sample	Species	Latitude	Longitude	Altitude	Aspect	Observations
IH01	*Nothofagus antarctica*	55°49.840'S	67°52.271'W	34 m	S	It presents signs of red lichens
IH02	*Nothofagus antarctica*	55°49.796'S	67°52.309'W	15 m	NE	Similar but it seems healthier
IH03	*Nothofagus antarctica*	55°49.843'S	67°52.289'W	28 m	SSE	Similar but it seems healthier
IH04	*Nothofagus antarctica*	55°49.845'S	67°52.296'W	31 m	SW	Similar with dead branches
IH05	*Nothofagus antarctica*	55°49.847'S	67°52.293'W	30 m	N	Similar but it seems health, with a lot of branches
IH06	*Nothofagus antarctica*	55°49.849'S	67°52.891'W	24 m	SE	Similar and main trunk is bended
IH07	*Nothofagus antarctica*	55°49.793'S	67°52.285'W	19 m	E	almost dead, just some leaves in the upper branches

Figure 37: Pictures of the individual tree core samples IH01-IH07.

10.2 Tree-ring width measurements of the samples
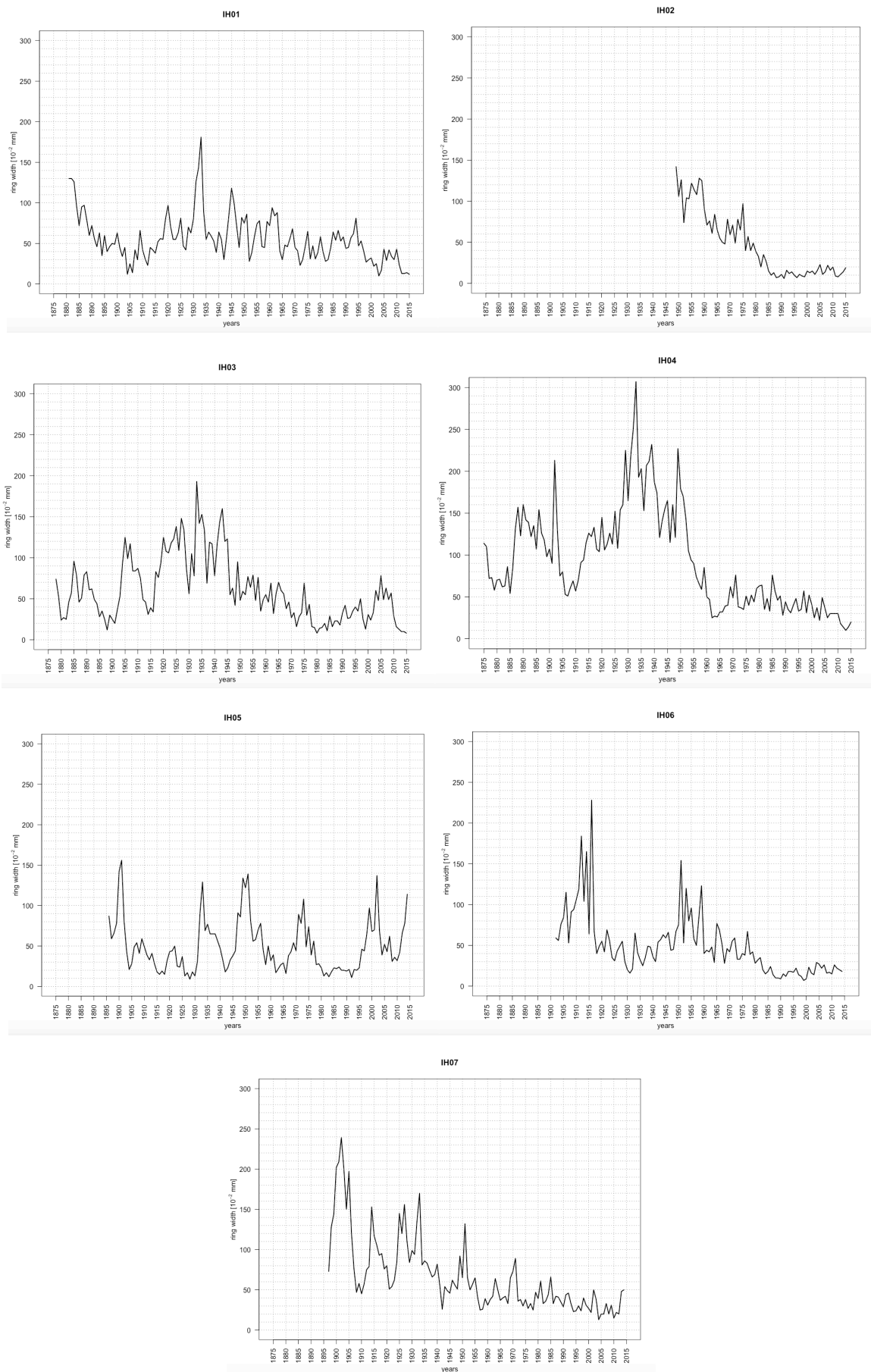
Figure 38: Individual measurements of the tree-ring width for the samples IH01-IH07.
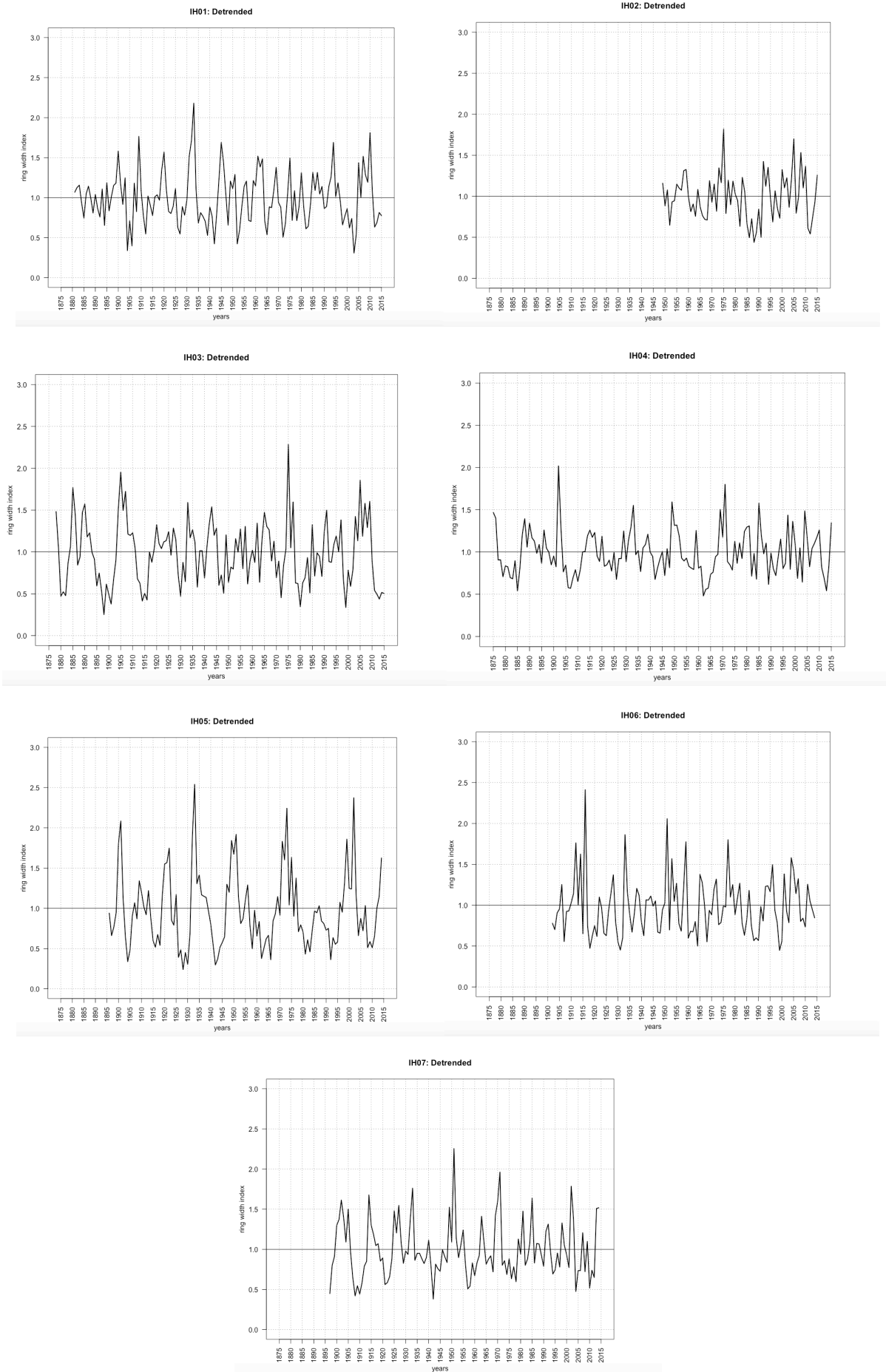
Figure 39: Detrended tree-ring width measurements for the samples IH01-IH07.

10.3 Laser ablation measurements

IH01: Sea salt relevant elements

IH03: Sea salt relevant elements
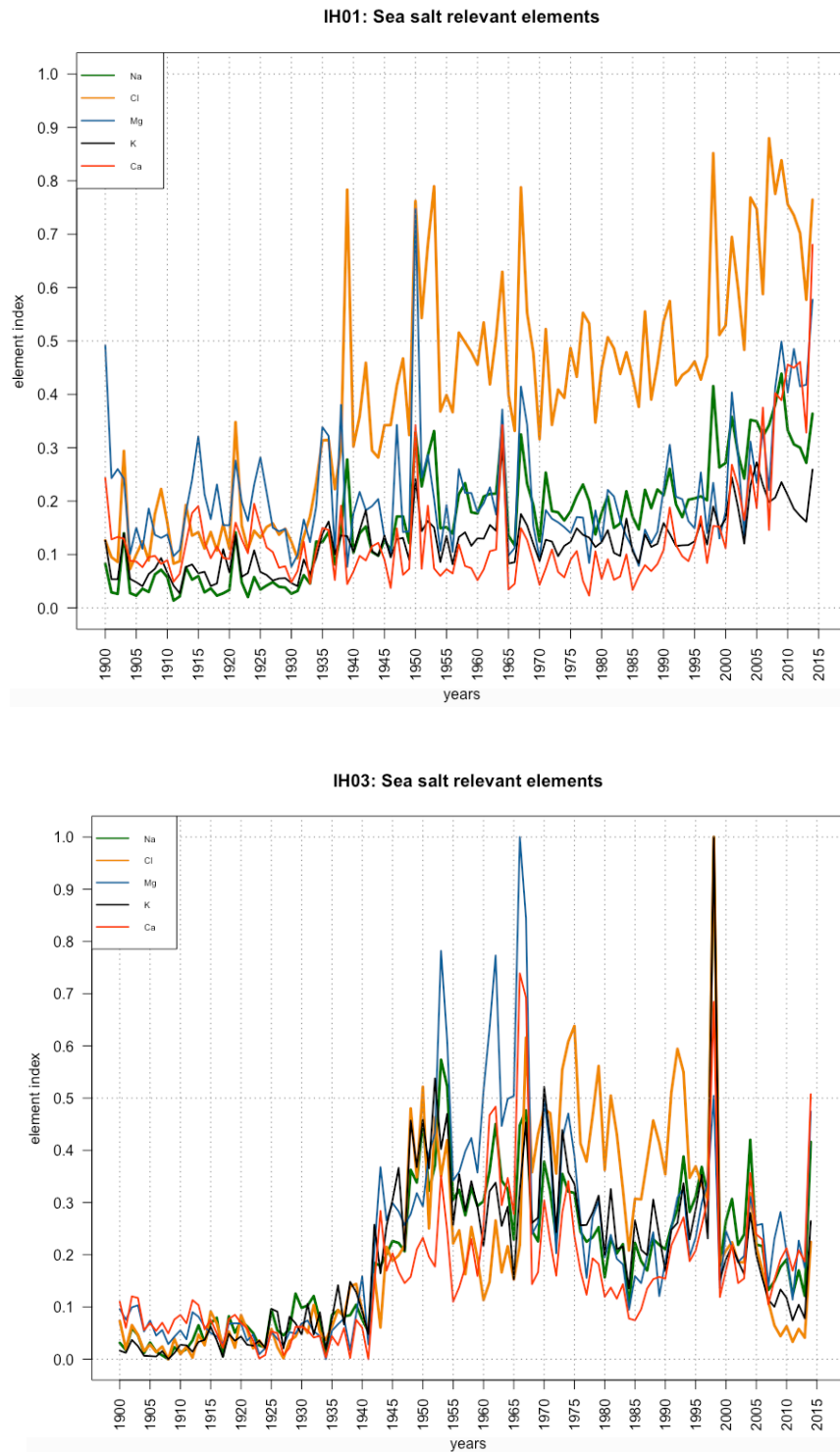
Figure 40: Detected sea seal relevant elements sodium (Na), chloride (Cl), magnesium (M), potassium (K) and calcium (Ca) for the samples IH01 and IH03 using laser ablation.

IH04: Sea salt relevant elements

IH05: Sea salt relevant elements
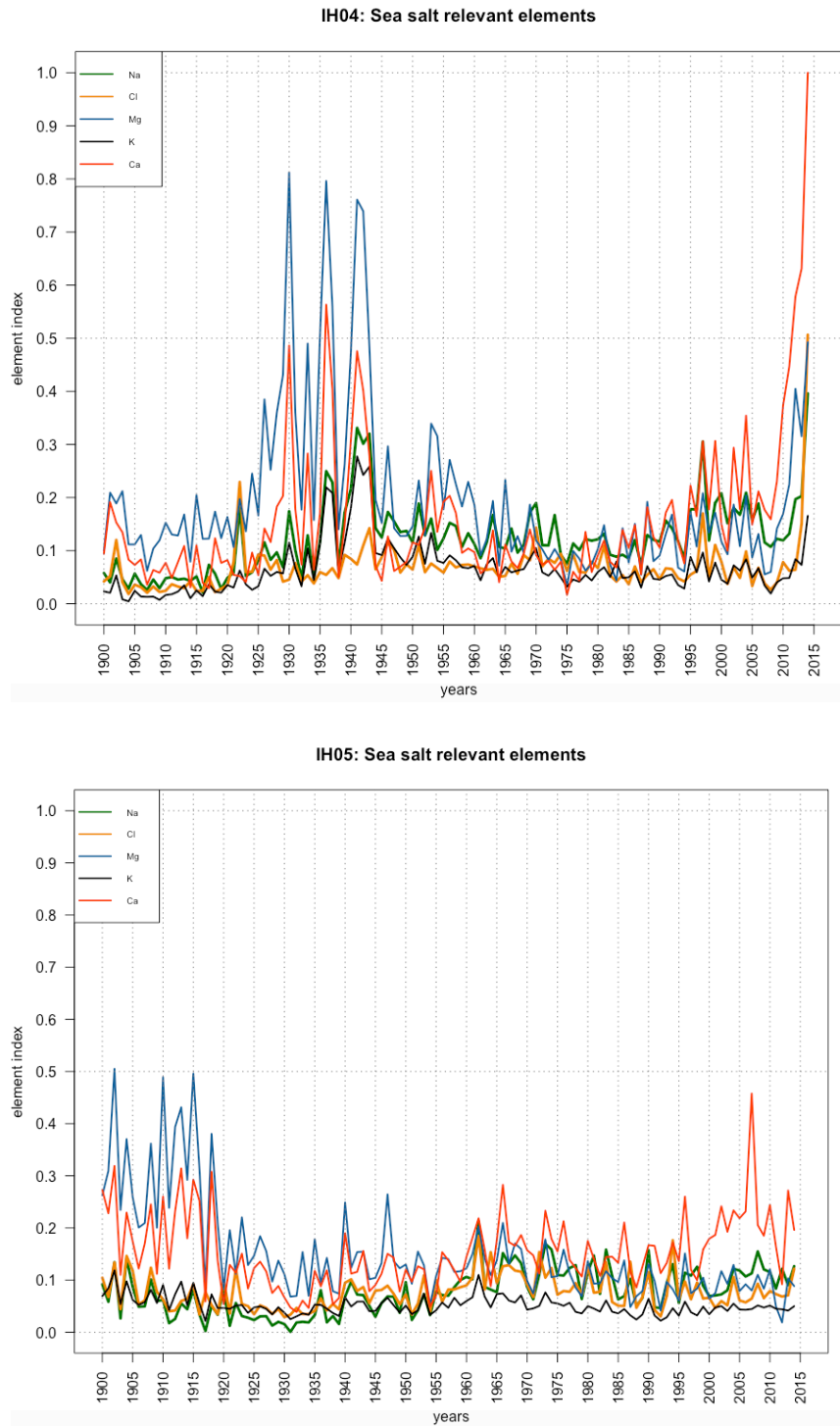
Figure 41: Detected sea seal relevant elements sodium (Na), chloride (Cl), magnesium (M), potassium (K) and calcium (Ca) for the samples IH04 and IH05 using laser ablation.

10.4 Correlations with wind relevant data and other SWW reconstructions

Analytical methods and SAM index
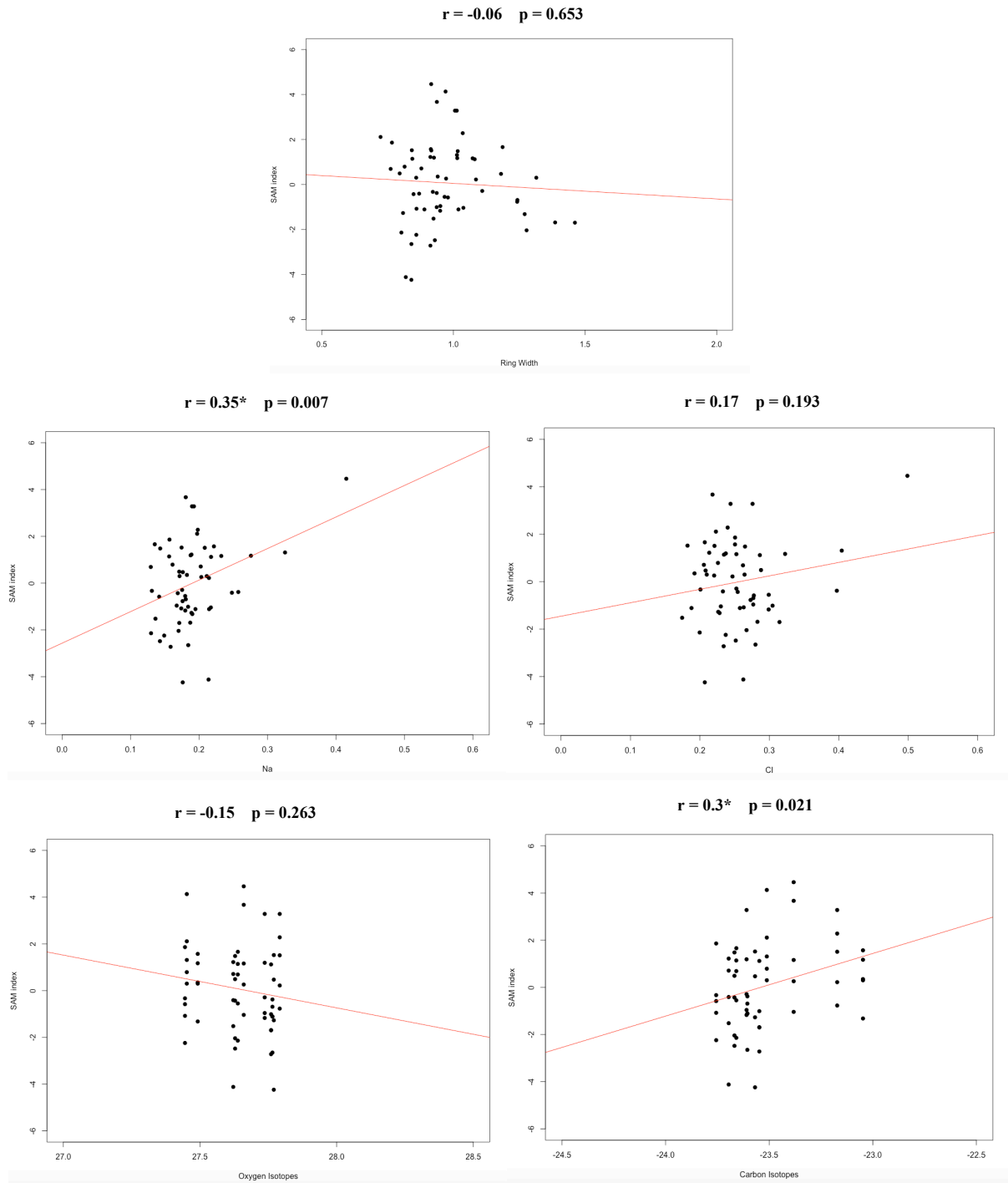
Figure 42: Scatterplots of the applied analytical methods (Na/Cl, oxygen/carbon isotopes) and SAM index. Significant moderate correlation is marked with * ($0.2 \leq |r| \leq 0.5$), significant good correlation with ** ($0.5 \leq |r| \leq 0.8$) and significant high correlation with *** ($0.8 \leq |r| \leq 1$). The significance level is $\alpha < 0.05$.

Analytical methods and wind speed of Ushuaia
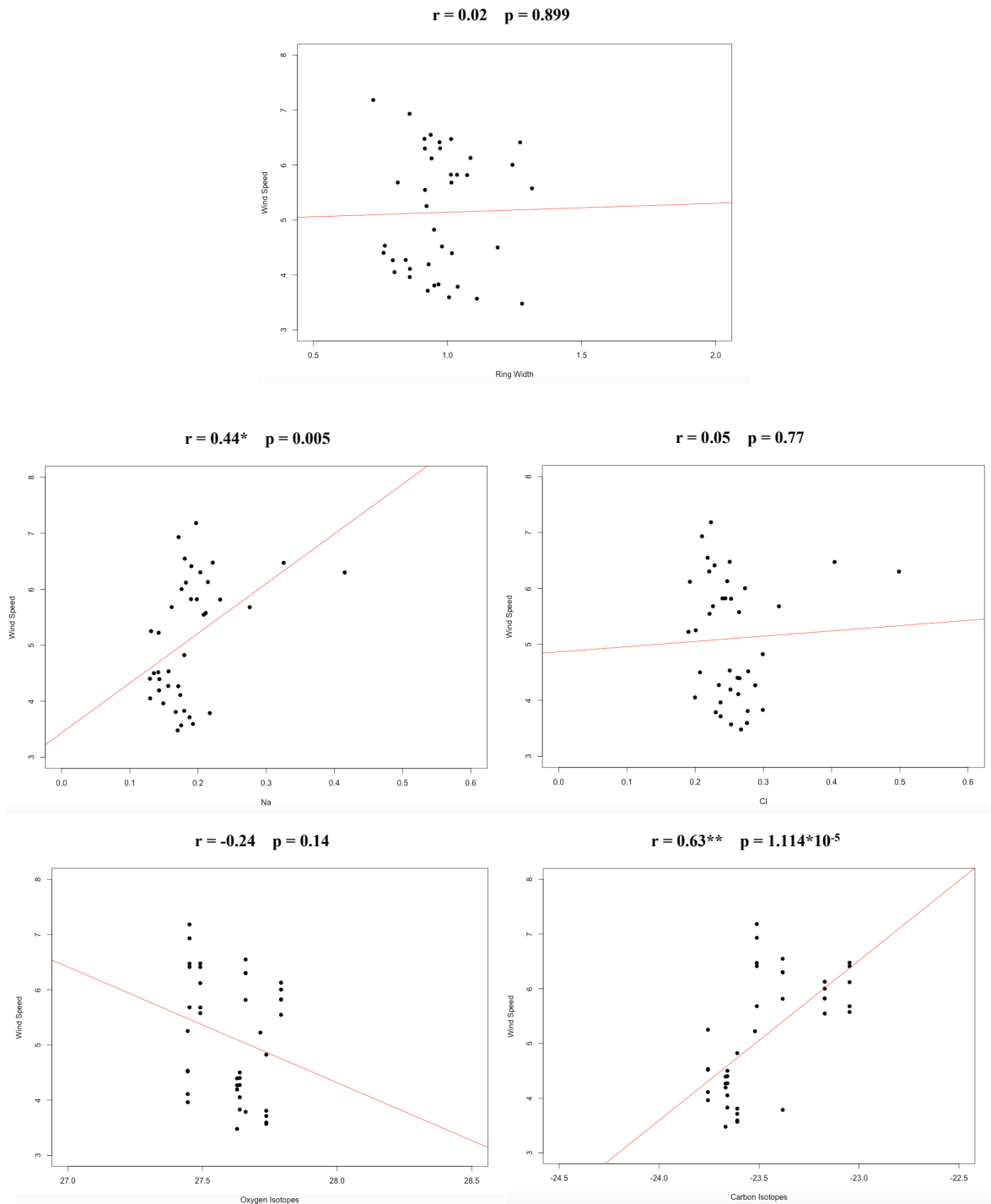
Figure 43: Scatterplots of the applied analytical methods (Na/Cl, oxygen/carbon isotopes) and wind speed measurements from the weather station in Ushuaia. Significant moderate correlation is marked with * ($0.2 \leq |r| \leq 0.5$), significant good correlation with ** ($0.5 \leq |r| \leq 0.8$ and significant high correlation with *** ($0.8 \leq |r| \leq 1$). The significance level is $\alpha < 0.05$.

Analytical methods and wind speed of Isla Hermite

r = -0.02   p = 0.808

r = 0.73   p < 2.2*10^{-16}**

r = 0.71   p < 2.2*10^{-16}**

r = -0.32*   p = 0.001

r = 0.27*   p = 0.004
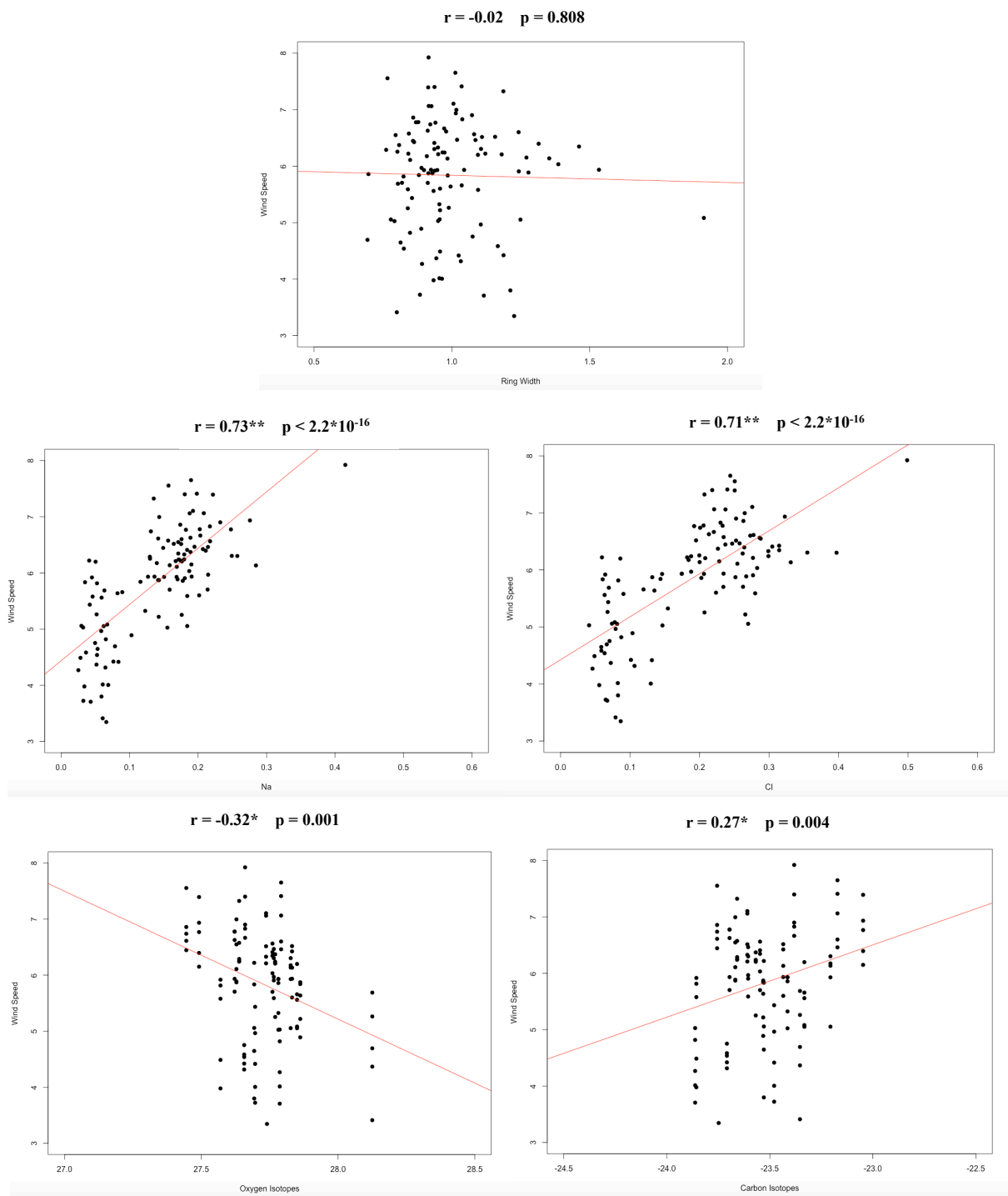
Figure 44: Scatterplots of the applied analytical methods (Na/Cl, oxygen/carbon isotopes) and reanalysis wind speed measurements around Isla Hermite. Significant moderate correlation is marked with * ($0.2 \leq |r| \leq 0.5$), significant good correlation with ** ($0.5 \leq |r| \leq 0.8$) and significant high correlation with *** ($0.8 \leq |r| \leq 1$). The significance level is $\alpha < 0.05$.

Tree-ring based SWW reconstructions with ice core based SWW reconstructions
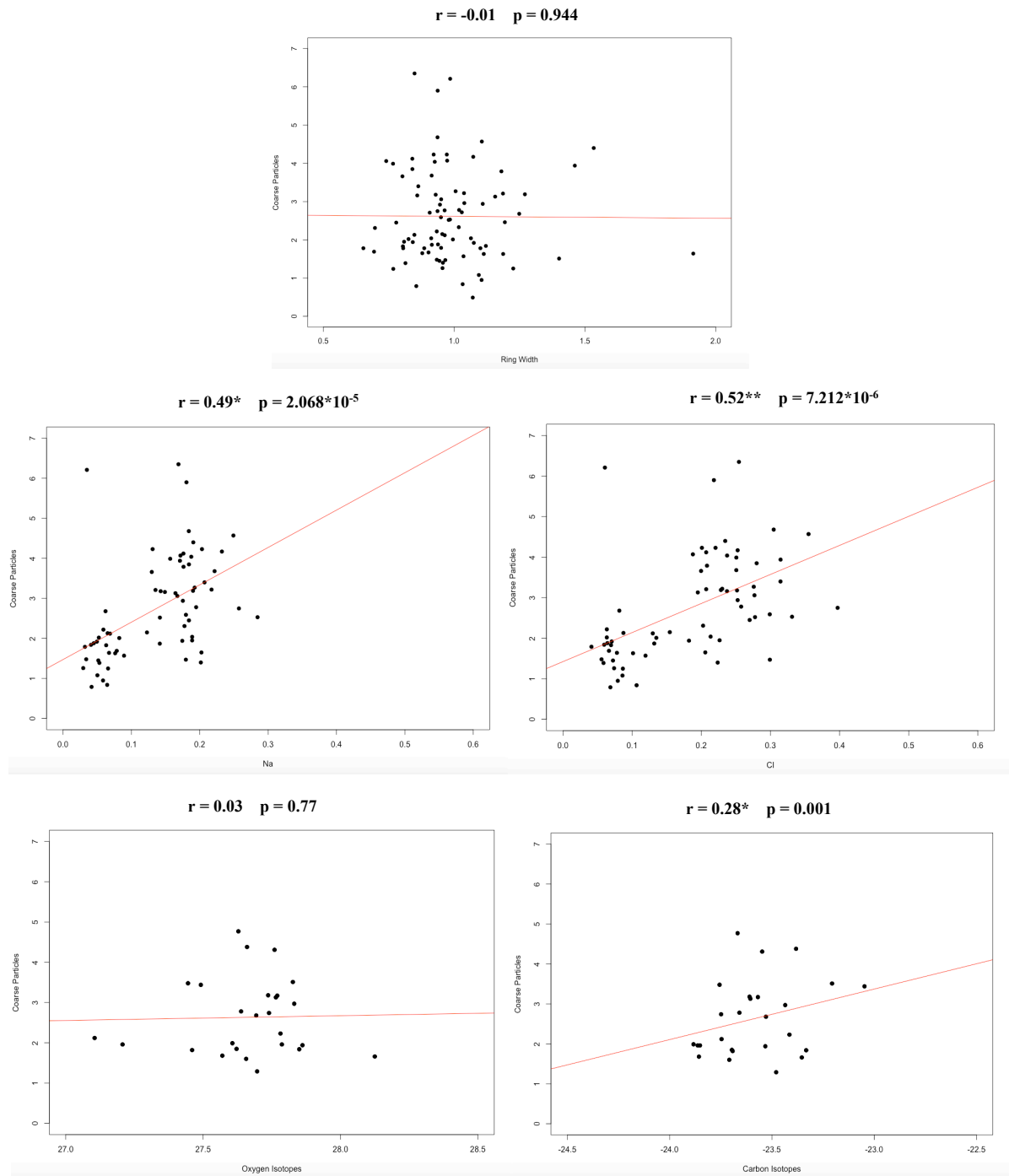
Figure 45: Scatterplots of the tree-ring based SWW reconstructions (Na/Cl, oxygen/carbon isotopes) and the WAIS ice cores-based Southern westerly winds reconstruction. For the isotopic data, also five year mean values were calculated for the coarse particles in the ice cores. Significant moderate correlation is marked with * ($0.2 \leq |r| \leq 0.5$), significant good correlation with ** ($0.5 \leq |r| \leq 0.8$) and significant high correlation with *** ($0.8 \leq |r| \leq 1$). The significance level is $\alpha < 0.05$.

11 Acknowledgements

12 Personal declaration

I hereby declare that the submitted thesis is the result of my own, independent work. All external sources are explicitly acknowledged in the thesis.

Zurich, 29.09.2020

....

(Michael Thomas Kessler)